Climate driven shifts in Southern Ocean primary producers and biogeochemistry in CMIP6 models

Ben J. Fisher[1], Alex J. Poulton[2], Michael P. Meredith[3], Kimberlee Baldry[4], Oscar Schofield[5], Sian F. Henley[1].

[1] School of GeoSciences, University of Edinburgh, Edinburgh, United Kingdom
[2] The Lyell Centre for Earth and Marine Science, Heriot-Watt University, Edinburgh, United Kingdom
[3] British Antarctic Survey, Cambridge, United Kingdom
[4] Institute for Marine and Antarctic Studies, College of Sciences and Engineering, University of Tasmania, Hobart, TAS, Australia
[5] Center of Ocean Observing Leadership, School of Environmental and Biological Sciences, Rutgers University, New Brunswick, NJ 08901, USA

Correspondence to: Ben J. Fisher (ben.fisher@ed.ac.uk)

Abstract. As a net source of nutrients fuelling global primary production, changes in Southern Ocean productivity are expected to influence biological carbon storage across the global ocean. Following a high emission, low mitigation pathway (SSP5-8.5), we show that primary productivity in the Southern Ocean is predicted to increase by up to 30% over the 21st century. The ecophysiological response of marine phytoplankton experiencing climate change will be a key determinant in understanding the impact of Southern Ocean productivity shifts on the carbon cycle. Yet, phytoplankton ecophysiology is poorly represented in Coupled Model Intercomparison 6 (CMIP6) climate models, leading to substantial uncertainty in the representation of their role in carbon sequestration. Here we synthesise the existing spatial and temporal projections of Southern Ocean productivity from CMIP6 models, separated by phytoplankton functional type, and identify key processes where greater observational data coverage can help to improve future model performance. We find substantial variability between models in projections of light concentration (>15000 ($\mu E\ m^2\ s^{-1}$)^2) across much of the iron and light limited Antarctic zone. Projections of iron and light limitation of phytoplankton vary by up to 10 % across latitudinal zones, while the greatest increases in productivity occurs close to the coast. Temperature, pH and nutrients are less spatially variable, projections for 2090-2100 under SSP5-8.5 show zonally averaged changes of +1.6 °C, -0.45 pH units and Si* ($[Si(OH)_4]– [NO_3^-]$) decreases by 8.5 μmol L^{-1}. Diatoms and pico-/miscellaneous phytoplankton are equally responsible for driving productivity increases across the Subantarctic and Transitional zones, but pico- and miscellaneous phytoplankton increase at a greater rate than diatoms in the Antarctic zone. Despite the variability in productivity with different phytoplankton types, we show that the most complex models disagree on the ecological mechanisms behind these productivity changes. We propose that a sampling approach targeting the regions with the greatest rates of climate-driven change in ocean biogeochemistry and community assemblages would help to resolve the empirical principles underlying phytoplankton community structure in the Southern Ocean.

1. Introduction

The biological uptake of carbon by marine phytoplankton represents an important process in the Earth system (Deppeler and Davidson, 2017), with ocean carbon storage mediating atmospheric CO_2 concentrations, including CO_2 of anthropogenic origin (Riebesell et al., 2007). Across the global ocean, uptake of carbon accounts for ~25% of CO_2 released by human activities (Friedlingstein et al., 2022). The Southern Ocean is a disproportionately large carbon and heat sink relative to its size (Frölicher et al., 2015), accounting for 30-40% of this global anthropogenic CO_2 uptake (e.g. Caldeira and Duffy, 2000;DeVries, 2014), predominantly due to enhanced atmosphere-ocean exchange at increased atmospheric CO_2 concentrations (Friedlingstein et al., 2022). While biological uptake is considered to play a minor role in total CO_2 uptake (Landschutzer et al., 2015;Gruber et al., 2019), variability in pCO_2 has been associated with summertime blooms in the Southern Ocean (Gregor et al., 2018;Coggins et al., 2023). Under a future climate scenario with longer growth seasons (Moreau et al., 2015), increased seasonal productivity (Leung et al., 2015;Fu et al., 2016) and a reduction in ocean CO_2 absorption efficiency (higher Revelle factor) (Hauck et al., 2015); biological and physical drivers of carbon exchange across the air-sea interface are likely to undergo substantial changes. As the Ocean's buffering capacity for increasing concentrations of atmospheric CO_2 reduces (Jiang et al., 2019), the role of pelagic ecosystems, are expected to become increasingly important in Southern Ocean carbon uptake (Henley et al., 2020).

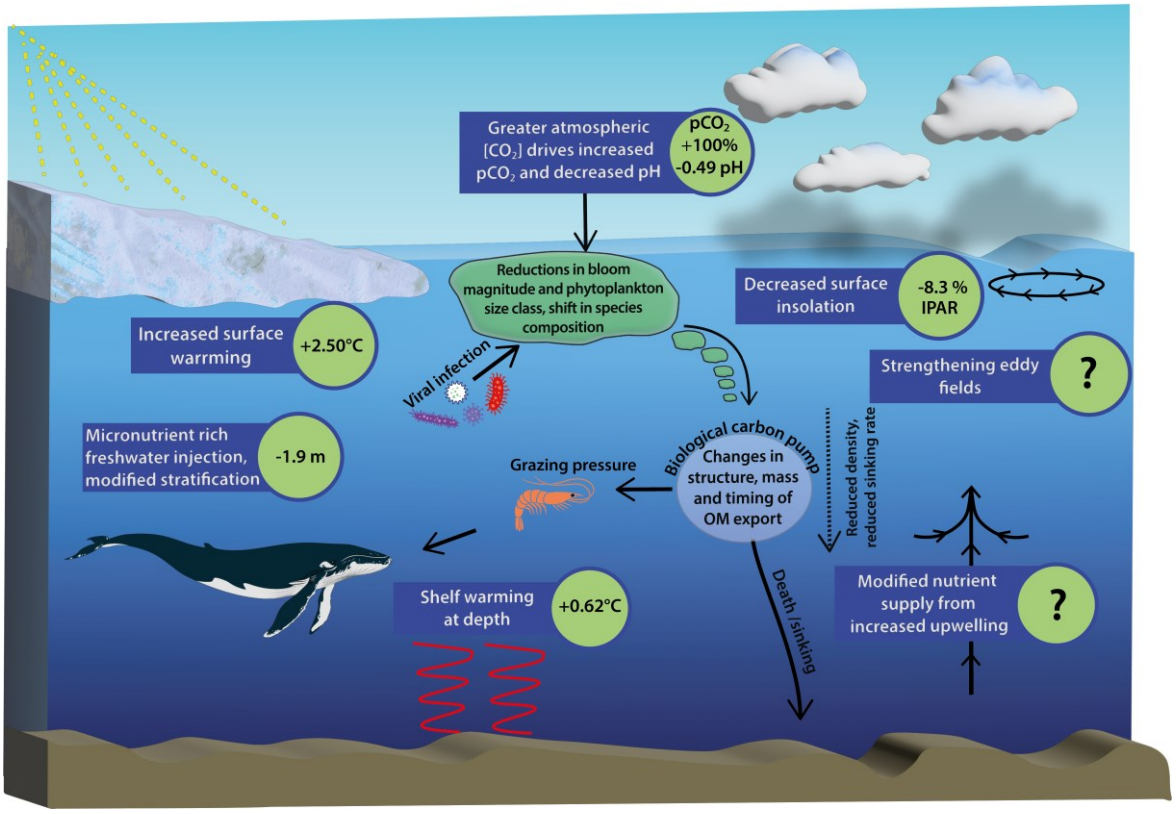

Figure 1: Schematic diagram of Southern Ocean pressures associated with climate change and the downstream biogeochemical consequences for ecosystem productivity. Values shown for surface warming, surface insolation and pH are 100 year mean changes to 2100 under the SSP5-8.5 scenario south of 65°S and are taken from CMIP6 models. Literature values are used for changes in pCO_2, stratification, and shelf warming at depth for the same time period and climate trajectory (Kawaguchi et al., 2013;Hauck et al., 2015;Purich and England, 2021) (see Table S1 for a full description). Question marks indicate key processes which drive biogeochemical change but are not currently included in CMIP models and therefore estimations of change do not currently exist.

Small celled marine phytoplankton (0.002-0.2 mm) are responsible for the production of biological carbon which fuels ecosystems, but are vulnerable to environmental change because of their specific requirements for light and iron, which are the primary factors limiting their growth in high nutrient low chlorophyll (HNLC) zones of the Southern Ocean (Moore et al., 2013). Following a "middle of the road" SSP2-4.5 pathway, being the scenario which mostly closely represents the current climate trajectory, between 2015 and 2023 Southern Ocean phytoplankton (defined as those south of 30°S per Gregg et al. (2003)) represented 36.31% of marine net primary productivity globally, equivalent to 15.5 Pg C yr^{-1} (Figure S1). Climate impacts on Southern Ocean phytoplankton are likely to manifest in ecological shifts towards smaller cell sizes (Venables et al., 2013;Saba et al., 2014;Schofield et al., 2018;Biggs et al., 2019;Mascioni et al., 2019) and changes in seasonal phenology (Moreau et al., 2015). Increases in overall productivity can be most closely associated with a reduced duration and extent of sea ice coverage, allowing for a greater supply of irradiance to surface waters of this light and iron co-limited productivity system. This increase in ocean surface area available for light transmission is offset by decreased insolation (-8.3%, Figure 1) associated with a greater degree of cloud cover. Strengthened upwelling is also likely to increase the flux of existing iron supplies to the coastal (Annett et al., 2015) and open ocean (Moreau et al., 2023) from sedimentary or hydrothermal sources, however, the extent to which changes in ocean mixing can be expected to impact nutrient supplies remains largely unknown (Figure 1).

Shifts in community composition from diatoms to smaller cryptophytes have already been documented along the West Antarctic Peninsula (Moline et al., 2004;Ducklow et al., 2007;Moline et al., 2008;Montes-Hugo et al., 2008;Rozema et al., 2017), and are thought to be due to tolerance of cryptophytes to the low-salinity waters induced by increased sea ice melt (Moline et al., 2004), or the tolerance of cryptophytes for high and variable light conditions in well stratified surface layers (Mendes et al., 2023). Conversely, in culture-based competition experiments, diatoms are more successful in simulated future ocean conditions over prevalent haptophytes such as *Phaeocystis antarctica,* albeit with reduced diatom cell sizes (Xu et al., 2014). This difference is potentially driven by reduced iron limitation of diatoms and their greater tolerance to temperature change (Zhu et al., 2016). These varied responses between manipulation experiments and *in situ* observations suggest that physiological, as well as ecological, adaptations are important in understanding the net biogeochemical implications of phytoplankton community change.

In the sea-ice zone, grazing by zooplankton accounts for ~90% of phytoplankton losses (Moreau et al., 2020). Shifts in phytoplankton size class could rapidly cascade through the ecosystem as the dominant Southern Ocean zooplankton, Antarctic krill (*Euphausia superba*, hereafter krill), are unable to graze small cryptophytes (Haberman et al., 2003). Instead this promotes

the growth of carbon-poor salps (*Salpa thompsoni*), which reduces the overall efficiency of the marine food web (Ballerini et al., 2014) and potentially weakens the biological carbon pump (Quéguiner, 2013;Biggs et al., 2021). Additionally, water temperature, alongside changes to zooplankton abundance and diversity, has been shown to increase zooplankton metabolism (Lopez-Urrutia et al., 2006;Mayzaud and Pakhomov, 2014), which can in turn be expected to modulate the grazing pressure and phytoplankton biomass (Lewandowska et al., 2014). Due to the strong relationship between temperature and metabolism in zooplankton, their abundance has been observed to follow the fronts of the Southern Ocean, with poleward contractions in salp and krill populations in response to warming (Constable et al., 2014;Atkinson et al., 2019).

Projections of productivity in the Southern Ocean under future climate scenarios from the Coupled Model Intercomparison Project Phase 6 (CMIP6) class Earth System Models (ESMs) are actively informing research directions, International Panel on Climate Change (IPCC) reports (Masson-Delmotte et al., 2021), and governmental policy (Touzé-Peiffer et al., 2020). Yet, between CMIP5 and CMIP6 the spread of model projections with respect to vertical and horizontal physics as well as the number of phytoplankton functional types included has increased as different models incorporate more complexity and additional processes (e.g., varying elemental stoichiometry, phytoplankton diversity, complex elemental cycling) (Seferian et al., 2020). While representation of ocean physical drivers and nutrient fields compared to observations has improved between CMIP5 and CMIP6, surface chlorophyll is one of three key parameters that did not show improvement in benchmarking of CMIP6 performance over the global ocean (Canadell et al., 2021;Fu et al., 2022). Variance in model projections of phytoplankton and ocean biogeochemistry have been linked to the use of fixed C:N:P elemental stoichiometry (Kwiatkowski et al., 2018), an inability to reflect physiological adaptations, e.g. the ability of diatoms to maintain growth under iron limitation (Person et al., 2018), and complexities in modelling export fluxes (Henson et al., 2022), particularly in constraining phytoplankton losses through zooplankton grazing (Cavan et al., 2017).

A major difference in the representation of productivity between CMIP6 models is the extent to which they consider different classes of phytoplankton. Diatoms (>20 μm) and pico-/nano-phytoplankton (predominantly cryptophytes and haptophytes) represent the vast majority of productivity across all latitudes of the Southern Ocean. Diatoms are a significant contributor to primary production and carbon export, accounting for ~40% of global marine primary production and POC exported to depth in the ocean (Jin et al., 2006;Tréguer et al., 2017). Diazotrophs (nitrogen-fixing phytoplankton) are present in small numbers, usually only in subtropical niches, due to the excess supply of nitrogen across the Southern Ocean (Luo et al., 2012). Calcifiers, mostly coccolithophores, inhabit waters north of 60°S where there is a strong supply of light but low Si, high Fe conditions, preventing the growth of diatoms (Charalampopoulou et al., 2016;Nissen et al., 2018). Only three CMIP6 models specifically include diatoms and pico-phytoplankton under future warming conditions (CESM2, CESM2-WACCM and GFDL-ESM4).

In recent years, record low sea ice concentrations have been observed in the Southern Ocean (Raphael and Handcock, 2022;Turner et al., 2022). Given the dependence of Southern Ocean productivity on the timing of seasonal sea ice retreat, we

consider it possible that this shift in trends of sea ice concentration could cause an abrupt change to sea ice dependent ecosystems in the near future (Swadling et al., 2023) . This is proposed to manifest in reduced algal, copepod, krill and fish populations with subsequent negative impacts on birds, mammals and associated ecosystem services (Steiner et al., 2021). As phytoplankton are the main source of organic carbon in the Southern Ocean, uncertainty in projections of phytoplankton composition compounds existing model uncertainty in the biological carbon flux to the ocean's interior and seafloor (Henson et al., 2022). Within the context of climate change in the Southern Ocean, reducing model uncertainty in ecosystem mediated biogeochemical cycling will be of increased importance in determining the global scale impact of changes in the Southern Ocean productivity regime.

In this study we aim to:

1. Quantify the degree of uncertainty between models in projections of phytoplankton productivity with a SSP5-8.5 warming scenario, including different phytoplankton functional types.
2. Determine mean trends between projected climate driven change in ecosystems, physical processes and biogeochemical cycling across different latitudinal zones of the Southern Ocean.
3. Identify regions, timeframes and processes within the Southern Ocean Observing System (SOOS) framework (https://soos.aq), where the greatest projected changes and/or uncertainties occur.

2. Methods

Model and observational data for the Southern Ocean were collected and visualised to determine a) the physical and biogeochemical changes that force or result from shifts in productivity, and b) the extent of primary productivity shifts over the next century in CMIP6.

2.1 CMIP projections

Model output was obtained from the Climate Model Intercomparison Project Phase 6 (CMIP6) data server via pangeo.io using the XMIP package in Python 3.11. Ensemble members for each parameter were chosen based on their availability for historical *(hist)* and SSP5-8.5 *(ssp585)* (ScenarioMIP) data (O'Neill et al., 2016). The selected models for each parameter are detailed in Table 1. Where an analysis type relied on the direct comparison between two or more parameters, only models that contained both parameters were selected. For the analysis presented in section 3.5, annual net primary production (*intpp*) is only included from models which also include diatom-specific annual net primary production (*intppdiat*) parameter. Where the same baseline model is included twice, because of having a low- and high-resolution version, the model is pre-averaged (i.e., both resolutions are assigned a weighting of 0.5 each) to avoid double counting of the same model when calculating the ensemble mean. Examples of models with two resolutions are highlighted in bold in Table 1. Only a small number of CMIP6 models contain irradiance limitation (*limirr*) and iron limitation (*limfe*) for multiple phytoplankton types, therefore analyses of light and iron

limitation of phytoplankton utilise <5 models. All variables were extracted at monthly frequency, except for surface wind speeds where data were initially obtained daily; subsequently, annual weighted means were generated for most parameters per the weighting algorithm by Grover (2021). For mixed layer depth and incidental photosynthetically active radiation (IPAR), austral summertime means were used instead of annual means.

Model data were processed in Python 3.11 to apply the desired analysis (e.g., annual average, annual maximum) and then further averaged over residual variables (e.g., member_id). In most cases, all available member_id's were used; where this was not possible, any member_id's which could not be aggregated due to differences in array structure were removed. Net primary production (NPP) is provided as a pre-integrated value across the water column; we integrated chlorophyll across the depth dimension between 0 and 500 m, to capture all phytoplankton across different depths, using the integrate function in SciPy (Virtanen et al., 2020). Subsequently, all models were re-gridded to a rectilinear grid via bilinear or nearest neighbour interpolation using XESMF (Zhuang et al., 2018) before being averaged to create multi-model means.

For spatial plotting, data were projected to the Antarctic Polar Stereographic (EPSG:3031) coordinate reference system in ArcGIS pro and visualised in QGIS using the Quantarctica package (Matsuoka et al., 2021), with post processing using SAGA and GDAL tools to remove imperfections in grid alignment through interpolation. All code to extract the CMIP6 data used in this study is available open access.

Table 1: Selected models used in analysis of CMIP6 data based on availability in the Pangeo catalouge. Models shown in bold represent multiple resolutions of the same core model which were subsequently averaged prior to calculation of the ensemble mean. Where direct comparisons are made between multiple parameters, ensembles were adjusted to include only those models which were existed for all of the selected parameters.

Variable ID	Parameter	Units	Data selection	Models selected
intpp	Primary organic carbon production by all types of phytoplankton / diatoms	gC m^{-2} yr^{-1}	Annual average	ACCESS-ESM1-5, CanESM5, CanESM5-CanOE, CESM2 CESM2-WACCM, CMCC-ESM2, CNRM-ESM2-1, EC-Earth3-CC, GFDL-ESM4, GFDL-CM4, IPSL-CM6A-LR, MIROC-ES2L, **MPI-ESM1-2-HR, MPI-ESM1-2-LR**, MRI-ESM2-0, **NorESM2-LM, NorESM2-MM**, UKESM1-0-LL
intppdiat				CanESM5-CanOE, CESM2-WACCM, CNRM-ESM2-1, GFDL-ESM4, IPSL-CM6A-LR , UKESM1-0-LL
chl	Mass concentration of total phytoplankton expressed as chlorophyll in sea water	kg m^{-3}	Annual average	ACCESS-ESM1-5, CanESM5, CanESM5-CanOE, CESM2, CESM2-WACCM, CMCC-ESM2, GFDL-CM4, GFDL-ESM4, MIROC-ES2L, **MPI-ESM1-2-HR**, **MPI-ESM1-2-LR**, MRI-ESM2-0, **NorESM2-LM**, **NorESM2-MM,** UKESM1-0-LL
limirrpico	Irradiance limitation of pico-phytoplankton / miscellaneous phytoplankton / diatoms/ diazotrophs	Ratio of growth under environmental irradiance to growth under unlimited irradiance	Annual average	CESM2-WACCM, GFDL-ESM4
limirrmisc				CanESM5, CNRM-ESM2-1,GFDL-ESM4, IPSL-CM6A-LR
limirrdiat				CESM2-WACCM, CNRM-ESM2-1, GFDL-ESM4, IPSL-CM6A-LR, UKESM1-0-LL
limirrdiaz				CESM2-WACCM, GFDL-ESM4

limfediat/pico/misc	Iron limitation of diatoms/picophytoplankton/ miscellaneous phytoplankton	Ratio of growth under environmental iron concentration to growth under unlimited iron concentration	Combined annual average	GFDL-ESM4
rsntds	Net Downward Shortwave Radiation at Sea Water Surface (IPAR)	W m^{-2} (Converted to µE m^{-2} s^{-1})	Summertime (daily) maximum	ACCESS-CM2, CanESM5, CanESM5-CanOE, CESM2-WACCM, CMCC-CM2-SR5, **CNRM-CM6-1**, **CNRM-CM6-1-HR**, CNRM-ESM2-1, EC-Earth3, EC-Earth3-CC, EC-Earth3-Veg, IPSL-CM6A-LR, MIROC-ES2L, **MPI-ESM1-2-HR**, **MPI-ESM1-2-LR**, **NorESM2-LM**, **NorESM2-MM**
sfcWindmax	Daily Maximum Near-Surface Wind Speed	m s^{-1}	Annual average of daily maxima	AWI-CM-1-1-MR, BCC-CSM2-MR, CanESM5, CMCC-CM2-SR5, CMCC-ESM2, **CNRM-CM6-1**, **CNRM-CM6-1-HR**, CNRM-ESM2-1, EC-Earth3, EC-Earth3-CC, **EC-Earth3-Veg**, **EC-Earth3-Veg-LR**, GFDL-CM4, HadGEM3-GC31-MM, INM-CM4-8, INM-CM5-0, IPSL-CM6A-LR, KACE-1-0-G, **MPI-ESM1-2-HR**. **MPI-ESM1-2-LR**, MRI-ESM2-0, UKESM1-0-LL
mlotst	Ocean Mixed Layer Thickness Defined by σ_t	m	Summertime maximum	ACCESS-CM2, BCC-CSM2-MR, CAMS-CSM1-0, CanESM5, CanESM5-CanOE, CESM2, CESM2-WACCM, CNRM-CM6-1, CNRM-ESM2-1, GFDL-ESM4, GISS-E2-1-G, HadGEM3-GC31-LL, IPSL-CM6A-LR, MPI-ESM1-2-HR, MRI-ESM2-0, NESM3, UKESM1-0-LL
phos	Sea surface pH	pH units	Annual average	CanESM5, CanESM5-CanOE, CESM2, CESM2-WACCM, GFDL-ESM4, IPSL-CM6A-LR, MIROC-ES2L, MRI-ESM2-0, NorESM2-LM

tos	Sea surface temperature	°C	Annual average	ACCESS-CM2, ACCESS-ESM1-5, BCC-CSM2-MR, CAMS-CSM1-0, CanESM5, CanESM5-CanOE, CESM2, CESM2-WACCM, CIESM, CMCC-CM2-SR5, CMCC-ESM2, **CNRM-CM6-1**, **CNRM-CM6-1-HR**, CNRM-ESM2-1, E3SM-1-1, EC-Earth3, EC-Earth3-CC, **EC-Earth3-Veg**, **EC-Earth3-Veg-LR**, FGOALS-f3-L, FGOALS-g3, FIO-ESM-2-0, GFDL-CM4, GFDL-ESM4, **HadGEM3-GC31-LL**, **HadGEM3-GC31-MM**, IITM-ESM, INM-CM4-8, INM-CM5-0, IPSL-CM6A-LR, KACE-1-0-G, KIOST-ESM, MCM-UA-1-0, MIROC6, MIROC-ES2L, **MPI-ESM1-2-HR**, **MPI-ESM1-2-LR**, MRI-ESM2-0, NESM3, **NorESM2-LM**, **NorESM2-MM**, TaiESM1, UKESM1-0-LL
sios	Surface concentration of silicic acid	µmol L^{-1}	Annual average	CanESM5-CanOE, GFDL-ESM4, IPSL-CM6A-LR, **MPI-ESM1-2-HR, MPI-ESM1-2-LR**, **NorESM2-LM, NorESM2-MM**, UKESM1-0-LL
no3os	Surface concentration of nitrate	µmol L^{-1}	Annual average	CESM2, CESM2-WACCM, GFDL-ESM4, NorESM2-LM, UKESM1-0-LL
limno3	Nitrate limitation of phytoplankton	Ratio of growth under environmental nitrate concentration to growth under unlimited nitrate concentration	Annual average	GFDL-ESM4

2.2 Regional data

Historical sea surface temperature and concentrations of surface nitrate and silicic acid were mapped from the World Ocean Atlas 2018 data product (Garcia et al., 2019), representing average values from 1955 to 2017 . For Si*, annually averaged data for nitrate and silicic acid were exported at a 1x1 degree resolution and subtracted from one another to produce Si*. Commonly observed marine variables (chlorophyll, temperature, nutrients, pH) were analysed by their regional sector using the Southern Ocean Observing System (SOOS) framework. The purpose of integrating CMIP6 projections within the main existing observation framework is to identify regions of the largest expected changes in routinely observed variables to inform the coordination of future sampling efforts by the SOOS regional working groups. Additionally, SOOS regions provide an additional quantification of heterogeneity of marine variables within the latitudinal zones. To determine Si*, pH, and temperature values by SOOS area, SOOS regions south of 55° were drawn as mask layers and subset using the zonal statistics function in QGIS.

3. Results and Discussion

3.1 Physical climate drives biological changes in Southern Ocean water masses

Climate change is driving substantial changes in Southern Ocean water masses (Bindoff et al., 2019). The widespread strengthening of Southern Ocean winds by up to 0.8 m s^{-1} (Figure 2a) and increased buoyancy fluxes (including freshwater inputs) act as opposing drivers of stratification, modifying mixed layer depth (Figure 2b). Mixed layers are projected to deepen across the Subantarctic by up to 10 m, but shoal across much of the rest of the Southern Ocean (Figure 2b). In light limited regions a shoaling of the mixed layer can be expected to increase productivity, as phytoplankton become concentrated closer to the surface, while in iron limited regions where iron is supplied by wintertime vertical mixing, deeper mixed layers can benefit depth integrated primary productivity by increasing the productive water volume over which iron concentrations are sufficient to promote growth (Llort et al., 2019) . Subsequently, the changing availability of light and iron across the Southern Ocean determines the abundance and composition of primary producers. Despite the importance of changes in Southern Ocean circulation for global ocean nutrient supply, the cumulative influence of physical processes across different spatial resolutions results in poor overall performance of CMIP-class models in this region when their historical runs are compared with observations (Meredith et al., 2019). A particular weakness of CMIP6 models is in reconstructing the sea ice changes that drive buoyancy forcing (Roach et al., 2020;Shu et al., 2020) which has an important role in determining the flux of heat and CO_2 across the ocean-atmosphere boundary. The uncertainty in sea ice change also results in a high degree of variation in coastal irradiance between models (Figure S2e), particularly for the Weddell Sea and Ross Sea regions. Recent large and unexpected changes in sea ice around Antarctica emphasise that greater knowledge of the key drivers and controls is required, in order to improve predictive skill in models (Turner and Comiso, 2017).

Across the Southern Ocean, the timing of the springtime onset of net primary production and the magnitude of summer biomass accumulation are controlled by light availability, as dictated by sea ice extent, cloud cover and water column structure (Henley et al., 2017). CMIP6 models project the greatest relative increase in productivity to occur across the coastal zone of the Southern Ocean (65-90°S) (Figure 2c, Figure S3), where irradiance limitation is reduced (Figure 2d). Conversely, across the Transitional zone (40-50°S), IPAR reduces (Figure 2e) with cloud cover driving changes in light beyond the sea ice zone, irradiance limitation increases (Figure 2d), and relative productivity increases are lesser here compared to the coastal Southern Ocean (Figure 2c, Figure S3). Increased iron limitation (Figure 2f) likely manifests from greater competition for iron driven by increased productivity (Figure 2c). This is despite a potential increase in iron supply with a deepening of the mixed layer across parts of the Subantarctic (50-65°S) (Figure 2b); brought about by reduced upper-ocean stratification from strengthening zonal winds (Carranza and Gille, 2015;Sallee et al., 2021). Increased iron limitation across much of the Antarctic and Subantarctic coincides with reduced light limitation (Figure 2d) beyond the region where IPAR increases (Figure 2e), this is consistent with greater iron demand from increased productivity (Figure 2c) driving phytoplankton to iron limitation before light limitation. Iron supply to the surface is subject to changes in the properties and movement of water masses, which lead to variable circulation strengths, depth boundaries, heat content and carbon sequestration resulting from climate-driven perturbations to the ice-ocean-atmosphere system (Bindoff et al., 2019;Meredith et al., 2019). Upwelling of nutrients and light availability for phytoplankton are both strongly influenced by mixed layer depth, which in turn varies seasonally with increased solar warming and ice melt driving deeper Southern Ocean pycnocline stratification through the summer (Sallee et al., 2021). Models generally agree on changes in summertime mixed layer depth across most of the open ocean (Figure S2b), the greatest source of uncertainty is at the terminus of the Ross (Ross Sea) and Flicher-Ronne (Weddell Sea) ice shelves. This uncertainty in stratification can be linked to the lack of representation of ice shelves and their meltwater flux in the current generation of CMIP models (Purich and England, 2021). Subsequently, the lack of a meltwater flux directly impacts biology and biogeochemical cycles through the absence of ice associated nutrient seeding (e.g. Death et al., 2014) alongside creating uncertainty in nutrient and light availability through an incomplete representation of stratification.

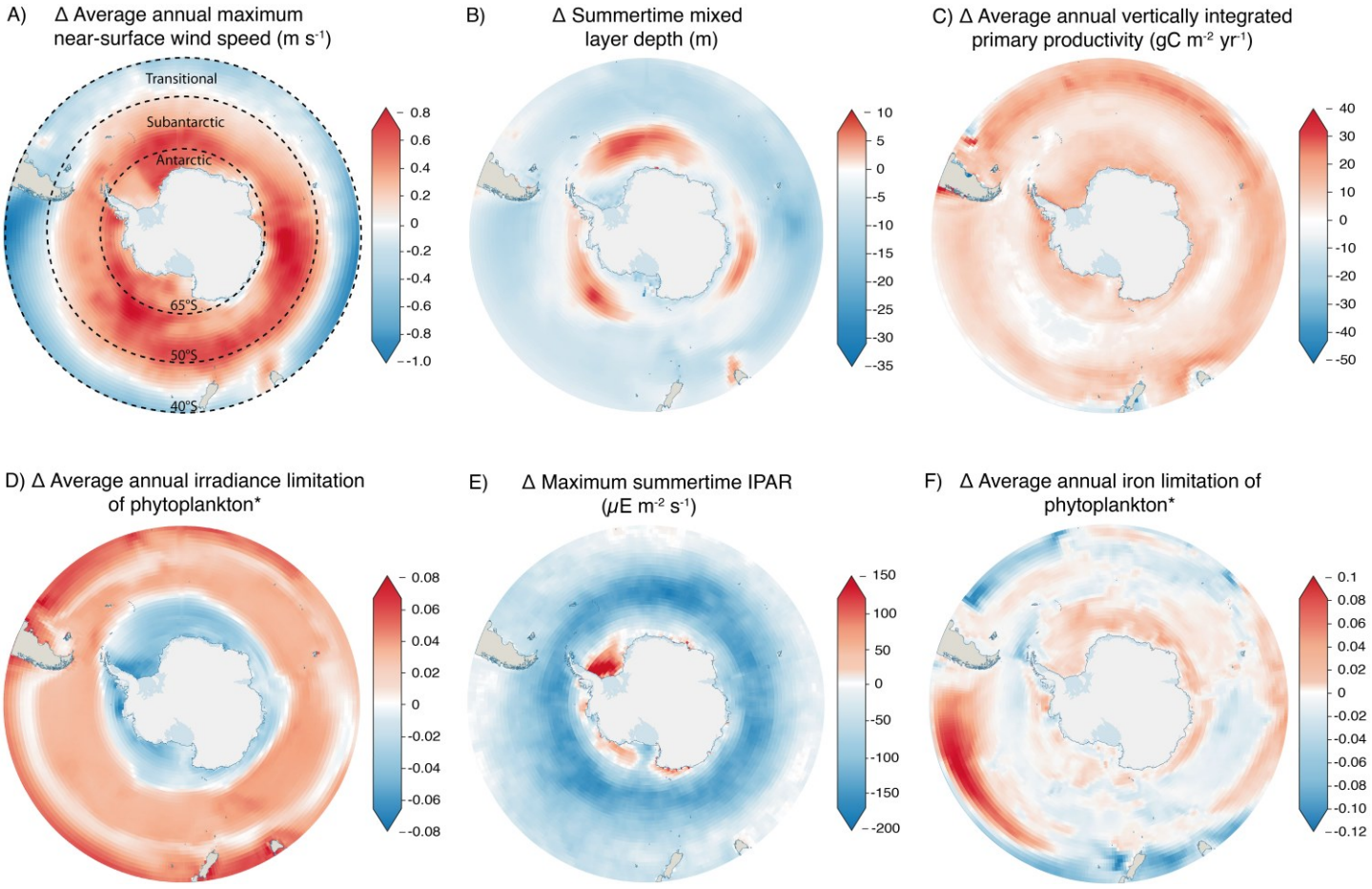

Figure 2: CMIP6 anomaly representing change to the end of the century in A) near-surface wind speed, B) mixed layer depth, C) net primary productivity, D) irradiance limitation of phytoplankton, E) incidental photosynthetically active radiation (IPAR), and F) iron limitation of phytoplankton. Changes are calculated from an ensemble of CMIP6 models, comparing a historical (1985-2015) average against 2090-2100 under the SSP5-8.5 climate scenario. Details of ensemble members are given in Table 1. *Units in panels D and F are arbitrary ratios of growth under environmental irradiance or iron concentrations against potential growth under unlimited irradiance or iron concentrations. Positive values represent an increase in limitation, while negative values represent a decrease in limitation. Latitudinal contours are shown for Figure 2a, these represent the northern boundaries of the Antarctic, Subtropical and Transitional zones.

3.2 Changing biogeochemistry of the Southern Ocean

3.2.1 Micronutrient supply and uptake

Iron acts as the primary limiting nutrient across the Southern Ocean (de Baar et al., 1995;Watson et al., 2000), due to supply limitation from low atmospheric inputs and significant distances from terrigenous sources (Boyd and Ellwood, 2010). Around the Antarctic coast, iron concentrations are set by processes including the resuspension of shelf sediments (Blain et al., 2001), and melting of sea ice (Lannuzel et al., 2016). The change in projected iron limitation of phytoplankton appears minimal (between -12 and 10% Figure 2f). Iron limitation is expected to increase most in the transitional zone between South America and New Zealand, correlating with a reduction in near-surface wind speed (Figure 2a), suggesting that atmospheric deposition of iron could decline in this region. There is a minor increase in iron limitation around the Antarctic coast, which represents the inverse of the decreasing trend in irradiance limitation (Figure 2d), indicating a shift towards an increasingly iron limited system, as reductions in sea ice concentrations increase light availability to coastal waters. The co-occurrence of an increase in iron limitation (Figure 2f) and an increase in total productivity (Figure 2c) across the coastal zone suggests that this increase in limitation is driven by an increase in the uptake of iron (from a larger productivity sink), as opposed to any substantial changes in supply.

Despite the importance of iron for phytoplankton growth in the Southern Ocean, CMIP series models have struggled to resolve the vertical supply of dissolved iron (Tagliabue et al., 2016), resulting in uncertainty for modelling primary and export productivity. At the group level, iron limitation could be expected to influence shifts in phytoplankton communities because larger cells may have a greater demand for iron compared to smaller cells (Hudson and Morel, 1990;Timmermans et al., 2004). In addition, other micronutrients such as manganese have been identified as a control on phytoplankton growth, particularly during seasonal transitions (Pausch et al., 2019;Browning et al., 2021;Balaguer et al., 2022), yet only iron is considered in ESMs, due at least partially to the lack of observational data to underpin distribution modelling of other micronutrients. Future work should continue to develop our understanding of the metabolic role of other micronutrients and additionally consider the extent to which diversity exists in micronutrient demand among Southern Ocean phytoplankton species.

3.2.2 Macronutrient supply and uptake

Nitrogen species, silicic acid (DSi) and phosphate are all essential for the growth and survival of diatoms, with nitrate and phosphate also being required by all other phytoplankton classes for cellular metabolism. Unlike much of the global ocean (Moore et al., 2013), high rates of macronutrient supply from the Circumpolar Deep Water (CDW) prevent widespread N or P limitation in the Southern Ocean except in periods of intense summer growth in high-productivity coastal regions (Henley et al., 2017). Although projections indicate an increase in chlorophyll across such regions (Figure 3), models do not show any

substantial increases in nitrate limitation south of the Subtropical zone over the remainder of the century (Figure S4), suggesting that iron and light will continue to be the primary constraints on productivity.

While macronutrients are not usually limiting to Southern Ocean phytoplankton, growth of diatom communities, particularly around high productivity coastal and island zones (supported by lateral iron advection) (Robinson et al., 2016), is likely to place an increased demand on DSi availability (Table 2). The relationship between Si and N is denoted as Si* (Sarmiento et al., 2004), with high Si* values (> 25) indicating plentiful DSi availability that supports diatom growth, while low values (< 10) suggest conditions which favour non-silicifying phytoplankton, such as the smaller cryptophytes and haptophytes. Si* is highest in the Antarctic zone (Henley et al., 2020) because of silica input from upwelling of CDW, but remains spatially heterogeneous within this region (Table 2). Si* is consistently high in the Weddell Sea, while across the WAP and Ross, Amundsen and Bellingshausen Seas there is a moderate mean Si* with large variability, and the Indian Sector has a substantially lower DSi availability. Si* is projected to decline by 2090-2100 at a zonally averaged value of -8.5 μmol L^{-1}, with the greatest declines being in the Ross and Weddell Seas, as well as the Indian sector (Table 2).

Decreases in Si* coincide with increases in chlorophyll concentration across the same regions (Figure 3), concurring with increased phytoplankton concentrations resulting in a drawdown of silicic acid. However, increases in chlorophyll appear independent from projected changes in primary productivity (Figure 2c). For example, the west Antarctic Peninsula and Amundsen Sea regions show the greatest increase in primary productivity, but are among the regions of smallest change for both Si* and chlorophyll. The divergence between chlorophyll and primary productivity indicates variability in Chl:C, with siliceous diatoms typically expressing more chlorophyll per unit of carbon (Sathyendranath et al., 2009). Therefore, the large chlorophyll increases and large Si* decline projected in the Weddell Sea are driven by an increase in diatoms (Figure S5), whereas the productivity increase with only small changes in both chlorophyll and Si* seen on the west Antarctic Peninsula result from an expansion of non-diatom phytoplankton with lower Chl:C (Figure S6).

The impact of climate change on DSi supply to the surface is difficult to evaluate because it is dependent on the competing stratification effects from wind driven changes to upwelling and an increase in freshening. Export of DSi from the surface and remineralisation at depth additionally act as important controls on supply; Freeman et al. (2018) showed that increased biological uptake of silicic acid, through increased diatom growth, leads to a poleward shift in the silicic acid front and a potential decoupling from the Antarctic polar front. Efforts to better define the nutrient budgets, particularly in increasingly common low sea ice years, across different sectors of the Southern Ocean, as well as understanding the changing nutrient demands of phytoplankton will be essential for determining future trends in nutrient limitation (Henley et al., 2019).

3.2.3 Ocean acidification

Across all regions of the Southern Ocean, continued uptake of anthropogenic CO_2 is expected to elicit a decrease in surface pH of ~0.45 units south of 55°S (Table 2) under the high emission scenario (SSP5-8.5). Projected changes in pH do not differ regionally, and show little variation within regions (low standard deviation), therefore regional changes in phytoplankton growth do not result from a direct acidification effect. In the CMIP6 models, phytoplankton growth is usually driven and limited by nutrients and light, while many models are built with complex carbonate systems, these typically only interact with rates of calcification and for the majority of phytoplankton there is no biotic feedback from changes to the carbonate system. This lack of biotic feedback prevents OA from impacting the main biological members of the Southern Ocean in CMIP6 despite expected acidification effects on diatom (Petrou et al., 2019), pico-phytoplankton (Tortell et al., 2008) and krill (Kawaguchi et al., 2013) populations. A more complex representation of phytoplankton-acidification effects in CMIP6 should include the interactive effect of acidification on phytoplankton stoichiometry, e.g., reduced silicification (Si:C) of diatoms Petrou et al. (2019). This change would allow OA to influence carbon export via modifying silicification, in addition to the existing modelled controls on phytoplankton silica content set by silicic acid and iron concentrations (Moore et al., 2004;Stock et al., 2014). Expanding model setups in CMIP6 to include the impact of OA and other physiochemical drivers on biogeochemical stoichiometry could help to resolve existing biases in Southern Ocean silicic acid concentrations (Long et al., 2021).

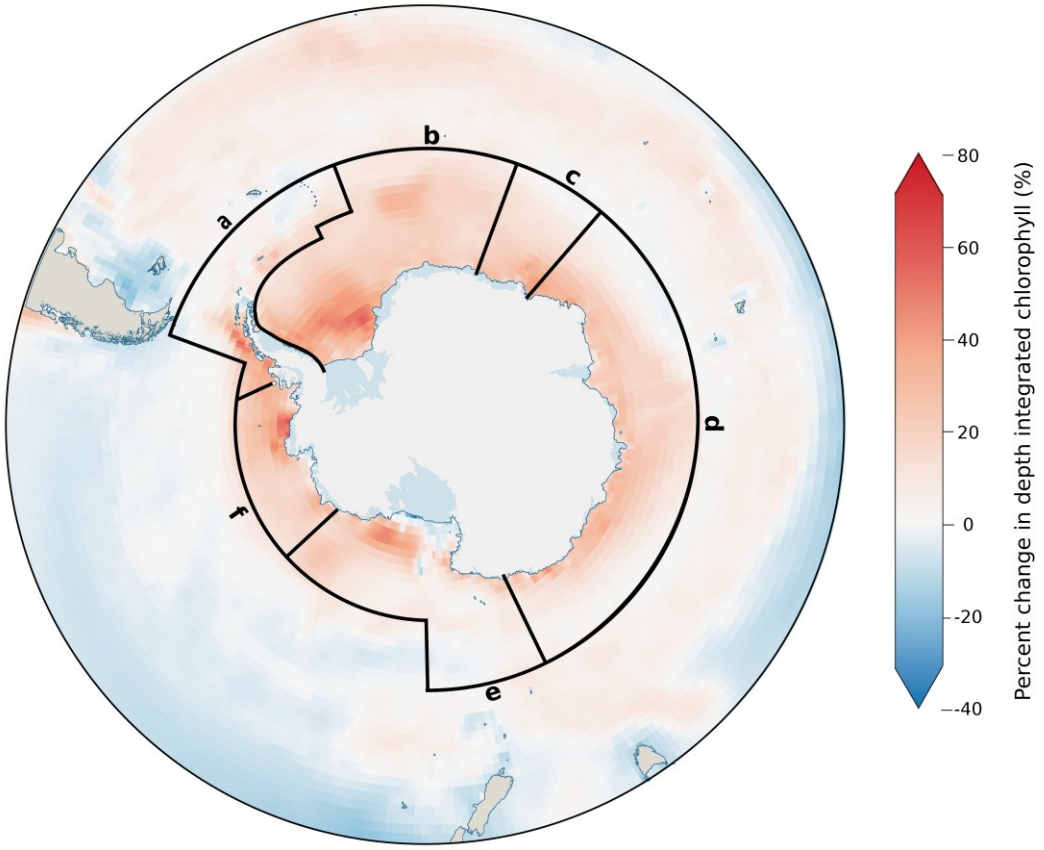

Figure 3: Change in depth-integrated chlorophyll (0-500 m) from all phytoplankton, displayed as the percentage change between the annual historical average (1985-2015) and projected values for 2090-2100. Values shown are multi-model means of the models listed in Table 1. Spatial boundaries show the Southern Ocean Observing System (SOOS) regions south of 55°S, which are defined in Table 2.

330

Table 2: Biogeochemical parameter values calculated for the Southern Ocean Observing System regions. SOOS regional working groups (as defined at: www.soos.aq/activities/rwg) indicated on Figure 3; section C is an overlap section of sections B and D. Data shown are: Si* ($[Si(OH)_4]$–$[NO_3^-]$) values and temperature determined from objectively analysed annual means of World Ocean Atlas 2018 data. pH was determined from a historical run of a multi-model ensemble of CMIP6 models (1985-2015). Delta values are anomalies of multi-
335 model means of pH, temperature and Si* based on comparisons between the mean annual historical value (1985-2015) and projected values for 2090-2100 under SSP5-8.5 for a CMIP6 ensemble (detailed in Table 1). Values in brackets are standard deviations, representing spatial variation across the region. Anomaly maps for pH, temperature and Si* are shown in Figure S7, S8 and S9 respectively.

Section	SOOS Region	Si* (µmol/L)	ΔSi*(µmol/L)	pH	Δ pH	Temperature (°C)	Δ Temperature (°C)
A	West Antarctic Peninsula & Scotia Arc	17.24 (17.82)	-7.06 (3.63)	8.07 (0.15)	-0.43 (0.01)	1.94 (1.87)	1.79 (0.37)
B	Weddell Sea & Dronning Maud Land (WSDML)	37.37 (9.70)	-10.98 (3.77)	8.08 (0.14)	-0.41 (0.01)	-0.07 (0.95)	1.43 (0.49)
C	SOIS/WSDML	23.16 (6.67)	-8.20 (1.59)	8.07 (0.01)	-0.41 (0.01)	1.08 (1.26)	1.89 (0.40)
D	Southern Ocean Indian Sector (SOIS)	4.71 (3.72)	-10.52 (3.67)	8.07 (0.13)	-0.41 (0.01)	1.78 (1.66)	1.78 (0.46)
E	Ross Sea	19.82 (18.49)	-9.13 (5.02)	8.08 (0.13)	-0.40 (0.02)	0.62 (2.22)	1.08 (0.46)
F	Amundsen and Bellingshausen Seas	17.59 (14.02)	-5.27 (4.33)	8.09 (0.16)	-0.43 (0.01)	0.11 (0.83)	1.73 (0.44)

3.3 Primary production and representation in CMIP6

340 Two CMIP6 models (GFDL-ESM4 and CESM2-WACCM) showed substantial mechanistic differences in productivity projections by phytoplankton type south of 65°S (Figure 4). While GFDL-ESM4 projects that in this region diatoms account for the majority (60%) of the change in productivity under SSP5-8.5 (Figure 4a,b), diatoms represent only 28% of the productivity increase in CESM2-WACCM, with pico-phytoplankton forming the major (72%) phytoplankton group (Figure 4e,d). Additionally, the GFDL model indicates that increased productivity is driven by increases in both diatoms and pico-
345 phytoplankton, representing a simultaneous growth scenario while CESM2-WACCM favours a replacement mechanism with

diatoms decreasing as pico-phytoplankton populations grow (Figure 4c,f). In CESM2-WACCM (MARBL biogeochemistry module) and GFDL-ESM4 (COBALTv2 biogeochemistry module), growth of phytoplankton groups is a product of temperature, nutrient limitation and light availability. In COBALTv2 the iron uptake half saturation constant is greater than in MARBL (0.1 vs 0.03 nmol kg^{-1} for small phytoplankton) and the differential between small and large phytoplankton (diatom) iron requirements is greater (x5 vs x2.3). Although phytoplankton in MARBL have lower Fe requirements, negative biases towards NO_3^- and PO_4^{-3} in the Southern Ocean by CESM2 suggest that NCP is overestimated, subsequently this could drive the system to iron limitation earlier, resulting in an "insufficient contribution from diatoms" (Long et al., 2021). This could suggest that GFDL-ESM4 presents a more realistic outlook for phytoplankton composition, however fixed nutrient constants which usually represent a global average collected from multiple studies, make no differentiation for changes to nutrient uptake in cold water environments. For example, Timmermans et al. (2004) showed iron uptake half saturation values for Southern Ocean diatoms to vary substantially between 0.19 and 1.14 nmol L^{-1} for different diatom species, compared to a fixed value of 0.5 nmol L^{-1} for COBALTv2 and 0.07 for MARBL, representing diatoms globally (Stock et al., 2020;Long et al., 2021). Experimentally, uptake half saturation constants are determined through the sequential addition of nutrients, yet multiple studies have shown that Southern Ocean diatoms in particular are able to reduce their cellular iron demand through changes to the photosynthetic pathway (e.g. Strzepek and Harrison, 2004;Jabre et al., 2021). Therefore, models based on these fixed constants may be reflecting the maximal iron uptake rather than the low iron acclimated uptake, i.e., this approach towards modelling nutrient limitation does not allow for a molecular adaptation which can, in some cases, achieve the same growth rate under more limiting conditions.

A shift from single species to community-based phytoplankton experiments for the purpose biogeochemical rates would help to improve our understanding of variability within the broad groups that exist for describing phytoplankton in CMIP6 models. For example, dynamic nutrient acquisition rates for different types of diatoms could replace a fixed nutrient half saturation constant for all diatom species if sufficient datasets existed to describe such rates at the species level. Developments of marine ecosystem models may include an expanded range of biological interactions such as group specific phytoplankton-zooplankton predation and bacterially-driven mixotrophic effects, such processes could alter trophic energy transfer and export fluxes through ESM's (Ward and Follows, 2016). Trait-based approaches have been explored as a means of modelling phytoplankton community composition, distinguishing functional groups based on life histories, morphology and physiology (Litchman and Klausmeier, 2008). Ocean biological sampling has some of the lowest coverage in the Southern Ocean (Sunagawa et al., 2020). Expansion of ecosystem observing at the metagenomics level (e.g., Guidi et al., 2016) offers a promising opportunity to expand our knowledge of traits and trade-offs in Southern Ocean phytoplankton communities, facilitating their integration into climate models.

In a changing ocean, phytoplankton will succeed where they have the greatest biological plasticity, for example the ability to photo-acclimate rapidly (Arrigo et al., 2010) or utilise a diverse range of nutrients (Kwon et al., 2022). The physiological

properties of any individual species ultimately determine their ability to survive in a particular region at a particular time under ever changing climate-driven conditions. Subsequently, species ecology determines the abundance and temporal extent with which a species can exist or compete in a particular region. As warming continues to bring about an earlier retreat of sea ice, growth seasons are expected to lengthen, altering the temporal dynamics of species progression (Moreau et al., 2015). In the coastal zone of the Southern Ocean, changes in light appear to be the main influence on productivity with decreased irradiance limitation stimulating pico-phytoplankton growth to a greater extent than diatoms (Figure 4 j,k,m,n); meanwhile iron limitation shows little correlation with productivity changes in this region with an R^2 of 0.51 for picophytoplankton and 0.06 for diatoms (Figure 4 g,h), likely because of replete iron supplies from coastal upwelling.

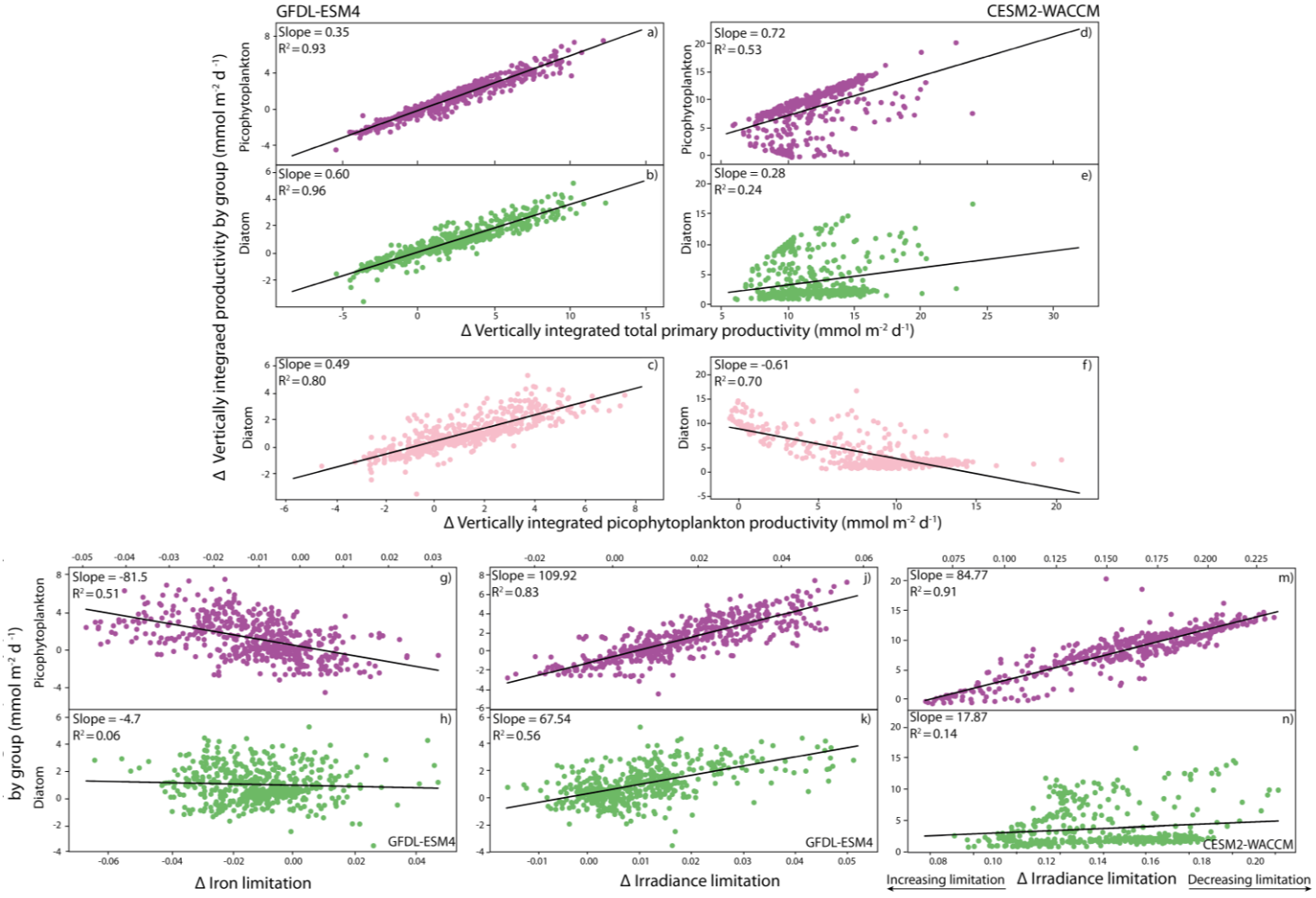

Figure 4: Evaluation of GFDL-ESM4 and CESM2-WACCM models using an anomaly between 2090-2100 (SSP5-8.5) and a historical average (1985-2015) for the Antarctic zone (65-90°S). Linear regression between change in total productivity and pico-phytoplankton productivity for GFDL-ESM4 (A) and CESM2-WACCM (D). Linear regression between change in total productivity and diatom productivity for GFDL-ESM4 (B) and CESM2-WACCM (E). Linear regression between change in picophytoplankton productivity and diatom productivity for GFDL-ESM4 (C) and CESM2-WACCM (F). Change in iron limitation with picophytoplankton (G) and diatom (H) productivity for GFDL-ESM4. Change in irradiance limitation with pico-phytoplankton (J) and diatom (K) productivity for GFDL-ESM4. Change in irradiance limitation with pico-phytoplankton (M) and diatom (N) productivity for CESM2-WACCM.

3.4 Latitudinal productivity projections in CMIP6.

From those models that do distinguish between at least diatoms and other phytoplankton we are able to examine projected changes in community composition over the 21st century under a continued warming scenario (SSP5-8.5) (Figure 5). Previous analysis by Laufkötter et al. (2015), using a different set of models (a mix of marine ecosystem models employed in CMIP5 and the Marine Ecosystem Model Intercomparison Project), found substantial disagreement between models in projecting which phytoplankton groups drove NPP changes in the Southern Ocean. In CMIP5, Leung et al. (2015) found a latitudinally banded response of phytoplankton to continued warming, driven by the bottom-up dynamics of nitrate, iron and light limitation. From this analysis, we applied the same latitudinal bands to our analysis of the changes in whole community, diatom and non-diatom productivity across CMIP6. Our whole community projections agree with the trends shown by Leung et al. (2015), of a poleward increase in phytoplankton productivity, increasing average total productivity south of 40°S, with increases in total productivity in the Transitional (40-50°S; Figure 5b), Subantarctic (50-60°S; Figure 5c), and Antarctic zones (65-90°S; Figure 5d). In relative terms, this reflects a ~10% increase in total productivity over the SSP5-8.5 run (2015-2100) for both the Transitional and Subantarctic zones, with a ~30% increase in productivity for the Antarctic zone (Figure S10 b,c,d). The poleward increases in productivity correlate with a deepening of mixed layers around the Antarctic zone (Figure 2b) and a reduction in coastal light limitation (Figure 2d), resulting in greater increases in Antarctic zone productivity compared to the Transitional or Subantarctic. An ensemble mean shows no overall change in productivity across the Subtropics (see also Tagliabue et al., 2021), however individual models show the widest degree of divergence in this region, with some models projecting decreases in the diatom population of over 60% (Figure S10a), indicating a large amount of uncertainty in the magnitude of productivity changes. Compositional changes in primary productivity across the subtropics are driven by reductions in nutrient availability from increased stratification (Fu et al., 2016) , as reflected in the increase in nitrate limitation across these regions (Figure S4). Under nutrient stress smaller phytoplankton can outperform larger phytoplankton, here diatoms, because of lower nutrient demands, leading to the modelled declines in diatom populations (Figure 7). The divergence in nutrient half saturation constants between different models (see 3.3) subsequently leads to a wide range of projections in species composition when nutrients become limiting.

In the Subantarctic (50-65°S), despite a large projected increase in light availability (Figure 2e), models project only a minor increase in productivity driven by a small amount of diatom growth, suggesting that growth of both diatom and non-diatom species remains largely iron-limited in this region. The coastal zone shows the greatest

degree of change in phytoplankton growth, with the largest increases in this region; the majority of the biomass change can be attributed to non-diatoms, however relative changes in both diatom and non-diatom populations are similar (Figure S10d), suggesting no overall changes to community composition here. The continued increase in all phytoplankton classes can be attributed to the decreased iron limitation across much of the zone (Figure 2f), with the success of non-diatoms reflecting the increase in light limitation (Figure 2d). Large phytoplankton types are more strongly affected by light limitation in CMIP6 because they have a greater requirement for light (as a lower constant for the chlorophyl specific initial slope of the photosynthesis-irradiance curve), in COBALTv2, large phytoplankton require 3x as much light as small phytoplankton to reach the same rate of photosynthesis (Stock et al., 2020). The lower requirements for iron and light by smaller phytoplankton types means that the change in relative abundance of smaller phytoplankton types to environmental change is often greater compared to diatom populations.

While CMIP6 models do not explicitly consider phytoplankton size, the shift from diatoms to, typically smaller, non-diatom species is consistent with more advanced ecological models such as DARWIN which predict a decrease in the slope of the phytoplankton size spectrum, albeit over a greater area of the Southern Ocean than shown in CMIP6 (Henson et al., 2021). Despite the clear differences between latitudinal bands, spatial heterogeneity continues to exist within these zones, particularly for the coastal zone where some of the greatest increases in chlorophyll occur in the WAP and Weddell Sea regions (Figure 3), reflecting the disproportionately high DSi supply in these regions (Table 2). Resolving spatial heterogeneity of phytoplankton in global-scale models such as those in CMIP6 is likely to require an increased reliance on, and integration with, regional-scale modelling (Person et al., 2018). The rapid increase of non-diatom species around the coast is in agreement with studies describing declining large diatom (>20 μm) abundances (Kang et al., 2001;Wright et al., 2010;Pearce et al., 2011); however, while it is true that diatoms are projected to decrease as a proportion of the community, diatom-derived carbon production is still projected to increase under continued warming, suggesting that the coastal biological carbon pump may be less threatened by this shift in community composition than previously thought.

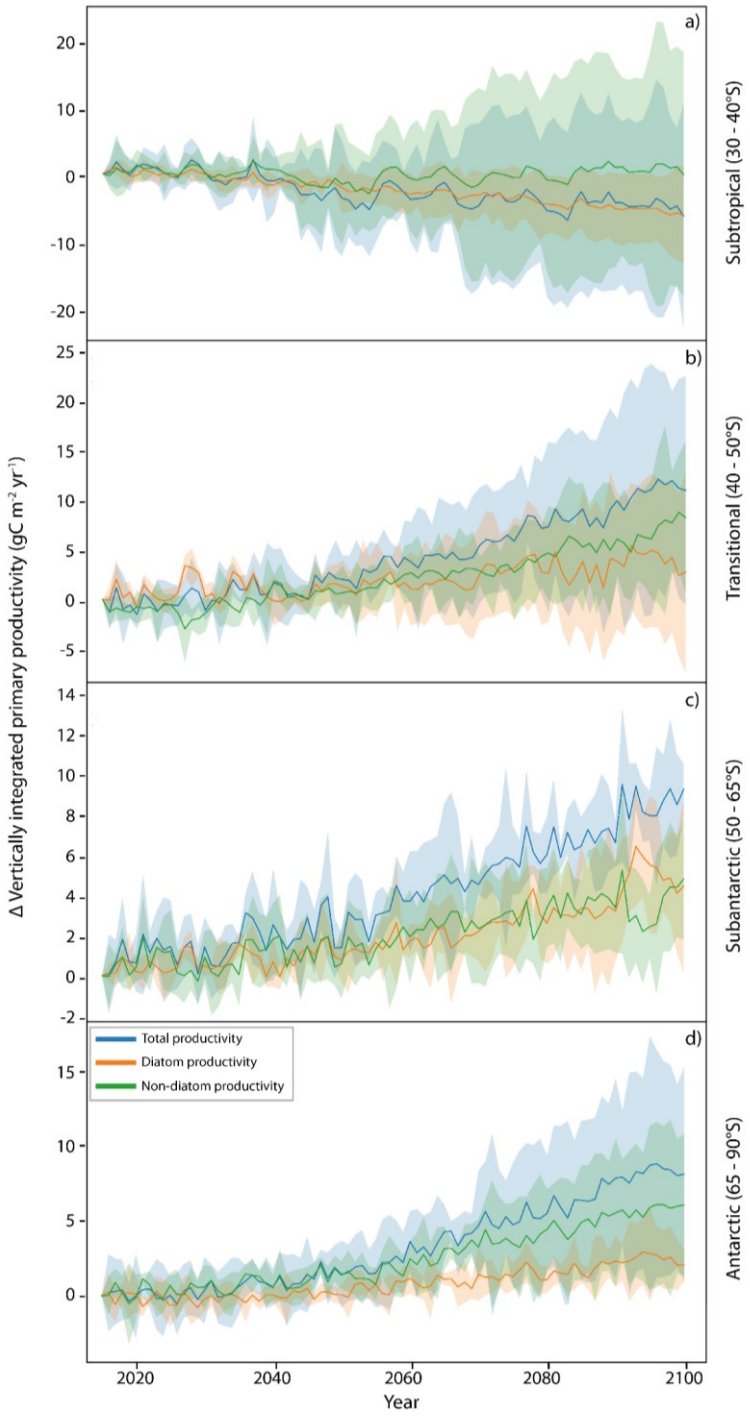

Figure 5: Changes in productivity (g C m^{-2} yr^{-1}) and the contribution of different phytoplankton classes to productivity, 2015-2100. The anomaly in CMIP6 model productivity projections (as POC production) compared to 2015 for SSP5-8.5 conditions spatially averaged across 4 latitudinal bands of the Southern Ocean, per Leung et al. (2015). Lines represent multi-model means of total productivity (intpp), diatom productivity (intppdiat) and non-diatom productivity (intpp-intppdiat). Shaded regions represent the spread between models as the interquartile range. Six CMIP6 models were used in this analysis, because only models containing the diatom productivity parameter are included; details of the specific models assessed are given in Table 1.

4. Conclusions

4.1 Implications of Southern Ocean productivity shifts

The cumulative impact of climate change on phytoplankton has the potential to restructure ecosystems of the Southern Ocean, with wider consequences for global ocean productivity and climate. In this study we found that CMIP6 models project a future Southern Ocean with increased levels of productivity, particularly around the Antarctic coastal zone. The major driver of this is reductions in light limitation, brought about by increased light concentrations from reduced sea ice coverage. However, the extent to which light will change is a source of great uncertainty, with the poor performance of sea ice also having additional implications for buoyancy forcing. Resolving freshwater fluxes from the Antarctic Ice Sheet could reduce model uncertainty in coastal mixed layer depth change. The current iteration of CMIP6 models do not suggest any significant shifts in the average community composition between latitudinal bands across the Southern Ocean, outside of a decrease in the relative abundance of diatoms in the subtropical zone. However, there is a large uncertainty of up to ± 30% for all phytoplankton classes across all zones of the Southern Ocean (Figure S10), and key processes which will impact phytoplankton (e.g., viral losses, composition of the grazer community) are absent from most models. A lack of complexity in the representation of zooplankton communities accounts for a large degree of uncertainty in phytoplankton composition and the marine carbon cycle (Rohr et al., 2023), this is particularly acute for the Southern Ocean where the major zooplankton fractions, salps and krill, feed on distinctly different size fractions of phytoplankton. However, Heneghan et al. (2023) find that within the context of climate change, uncertainty in Southern Ocean phytoplankton distributions in a warmer ocean lead to uncertainty in future zooplankton projections. Improving the predictive skill of CMIP6 models for Southern Ocean phytoplankton could therefore unlock mutual benefits for increasing the accuracy of zooplankton model outputs.

In models which do separate productivity by phytoplankton type, the growth of one type of phytoplankton over another is a product of light, temperature and nutrient limitation. Fixed nutrient stoichiometry is a key limitation in projecting phytoplankton composition, in particular the lack of interaction between physiochemical processes such as OA with biogeochemistry could be responsible for some of the existing biases in models towards excess Si in the Southern Ocean. We showed that for two models (GFDL-ESM4 and CESM2-WACCM) the iron requirements of different phytoplankton types can result in either a simultaneous growth of diatoms and picophytoplankton, or a replacement of diatoms with picophytoplankton. Future model generations might consider the acclimation of diatoms to low iron conditions, models currently use very different uptake half saturation values for iron, which disproportionally impacts community composition in iron limited regions. However, the literature also contains wide divergence in experimentally determined nutrient uptake constants (see 3.3), a more accurate approach towards modelling will first require us to better define what drives this variability in iron requirements. With continued record low sea ice trends, observation of phytoplankton responses in this multi-stressor environment will be

essential in understanding the scale of productivity change occurring and provide a basis to incorporate phytoplankton community change into global scale modelling efforts.

4.2 Observational recommendations:

Opportunities to improve the representation of Southern Ocean biogeochemical processes in CMIP encountered in this paper can be grouped in to three approaches: a) the addition of currently unrepresented physical processes b) increasing the complexity of existing biological processes, and c) by updating values used as constants in existing model processes to reflect regional variability (e.g., Southern Ocean specific nutrient half saturation constants). Observational monitoring is crucial for developing the evidence based required to improve the representation of temporal (e.g., nutrient fluxes from AIS melt), spatial (e.g., biogeochemical impacts of eddies) and biological (e.g., integrating size specific metrics for zooplankton rates, traits and stocks (Ratnarajah et al., 2023)) variability for incorporation into models. Within this resource limited environment, this study sought to identify regions with the largest expected changes and uncertainties in biogeochemically linked parameters as targets for future observational work. By monitoring change across these suggested target regions, we can a) supplement existing data sets to reduce the range of uncertainties and b) use areas of extreme projected change as test beds for mechanistic studies to identify critical thresholds and tipping points in biogeochemical relationships.

For phytoplankton groups, the largest degree of uncertainty is in the abundance of diatoms and non-diatoms between 40°S and 65°S. This is particularly acute for diatom abundance across the Transitional zone where the scale of uncertainty spans positive and negative values for most of the present century. Within the models, spatial variability in Transitional zone diatom populations correlates with changes to nitrate limitation. Areas of the transitional zone which are close to land also account for the largest uncertainties in model ensemble projections of primary productivity (>1000 $gC\ m^2\ yr^{-1}$). The concentration of nitrate across the lower latitudes in regions close to land should be a key priority for observation as this will inform our understanding of the viability of diatom populations in the lower latitudes and reduce the ~60% uncertainty in the modelled poleward movement of diatom communities towards the Subantarctic under climate change. Across the Subantarctic, the largest increases in diatom populations are projected to occur over the SOOS Southern Ocean Indian Sector (SOIS), a region which is poorly studied relative to the WAP and Weddell and Ross seas. Improving the coverage of phytoplankton community composition studies in the SOIS could be most fruitful in observing the movement of diatoms between latitudinal zones. Meanwhile, the largest relative change in productivity (>200%) is expected to occur across the Weddell Sea, this could make the Weddell Sea an increasingly important observational target for the mechanistic study of wider ecosystems, including zooplankton grazing patterns on different phytoplankton types. From the identification of these trends in the CMIP6 model ensembles, we propose that model projections could be used to target our observational capacity towards regions where enhanced data collection would be most beneficial in reducing uncertainties and ground-truthing expected rates of change. Consequently, this would strategically increase our evidence base to fill data and process knowledge gaps and inform future

generations of ESM projections, improving our ability to project and observe biogeochemical change across the Southern Ocean in response to climate change.

Acknowledgements

BJF is supported by a NERC Doctoral Training Partnership Grant (NE/S007407/1). SFH would like to acknowledge support from NERC (NE/K010034/1). This work used JASMIN, the UK's collaborative data analysis environment (https://jasmin.ac.uk). For the purpose of open access, the author has applied a creative commons attribution (CC BY) licence to any author accepted manuscript version arising.

Data availability

CMIP6 data were obtained through, and are freely available at panego.io. Specific models and parameters extracted for each analysis are listed in Table 1. Code for CMIP6 data analysis are available at: *(zenodo link to be later inserted, available to reviewers as attached zip file)*.

Author contributions

BJF, SFH, MPM and AJP devised the concept for the paper and contributed towards initial drafting and editing. BJF performed model analysis and produced the figures. OS and KB provided input on conceptual design and edited previous versions of the manuscript. All authors have approved the final version of the manuscript.

Competing interests

The authors declare no competing interests.

References

Annett, A. L., Skiba, M., Henley, S. F., Venables, H. J., Meredith, M. P., Statham, P. J., and Ganeshram, R. S.: Comparative roles of upwelling and glacial iron sources in Ryder Bay, coastal western Antarctic Peninsula, Marine Chemistry, 176, 21-33, 10.1016/j.marchem.2015.06.017, 2015.

Arrigo, K. R., Mills, M. M., Kropuenske, L. R., van Dijken, G. L., Alderkamp, A. C., and Robinson, D. H.: Photophysiology in two major southern ocean phytoplankton taxa: photosynthesis and growth of Phaeocystis antarctica and Fragilariopsis cylindrus under different irradiance levels, Integr Comp Biol, 50, 950-966, 10.1093/icb/icq021, 2010.

Atkinson, A., Hill, S. L., Pakhomov, E. A., Siegel, V., Reiss, C. S., Loeb, V. J., Steinberg, D. K., Schmidt, K., Tarling, G. A., and Gerrish, L.: Krill (Euphausia superba) distribution contracts southward during rapid regional warming, Nature Climate Change, 9, 142-147, 2019.

Balaguer, J., Koch, F., Hassler, C., and Trimborn, S.: Iron and manganese co-limit the growth of two phytoplankton groups dominant at two locations of the Drake Passage, Commun Biol, 5, 207, 10.1038/s42003-022-03148-8, 2022.

Ballerini, T., Hofmann, E. E., Ainley, D. G., Daly, K., Marrari, M., Ribic, C. A., Smith, W. O., and Steele, J. H.: Productivity and linkages of the food web of the southern region of the western Antarctic Peninsula continental shelf, Progress in Oceanography, 122, 10-29, 10.1016/j.pocean.2013.11.007, 2014.

Biggs, T. E. G., Alvarez-Fernandez, S., Evans, C., Mojica, K. D. A., Rozema, P. D., Venables, H. J., Pond, D. W., and Brussaard, C. P. D.: Antarctic phytoplankton community composition and size structure: importance of ice type and temperature as regulatory factors, Polar Biology, 42, 1997-2015, 10.1007/s00300-019-02576-3, 2019.

Biggs, T. E. G., Huisman, J., and Brussaard, C. P. D.: Viral lysis modifies seasonal phytoplankton dynamics and carbon flow in the Southern Ocean, ISME J, 15, 3615-3622, 10.1038/s41396-021-01033-6, 2021.

Bindoff, N. L., Cheung, W. W., Kairo, J. G., Arístegui, J., Guinder, V. A., Hallberg, R., Hilmi, N. J. M., Jiao, N., Karim, M. S., and Levin, L.: Changing ocean, marine ecosystems, and dependent communities, IPCC special report on the ocean and cryosphere in a changing climate, 477-587, 2019.

Blain, S., Tréguer, P., Belviso, S., Bucciarelli, E., Denis, M., Desabre, S., Fiala, M., Jézéquel, V. M., Le Fèvre, J., Mayzaud, P., Marty, J. C., and Razouls, S.: A biogeochemical study of the island mass effect in the context of the iron hypothesis:: Kerguelen Islands, Southern Ocean, Deep-Sea Research Part I-Oceanographic Research Papers, 48, 163-187, Doi 10.1016/S0967-0637(00)00047-9, 2001.

Boyd, P. W., and Ellwood, M. J.: The biogeochemical cycle of iron in the ocean, Nature Geoscience, 3, 675-682, 10.1038/ngeo964, 2010.

Browning, T. J., Achterberg, E. P., Engel, A., and Mawji, E.: Manganese co-limitation of phytoplankton growth and major nutrient drawdown in the Southern Ocean, Nat Commun, 12, 884, 10.1038/s41467-021-21122-6, 2021.

Caldeira, K., and Duffy, P. B.: The role of the southern ocean in uptake and storage of anthropogenic carbon dioxide, Science, 287, 620-622, 10.1126/science.287.5453.620, 2000.

Canadell, J. G., Monteiro, P. M., Costa, M. H., Da Cunha, L. C., Cox, P. M., Alexey, V., Henson, S., Ishii, M., Jaccard, S., Koven, C., Lohila, A., Patra, P. K., Piao, S., Rogelj, J., Syampungani, S., Zaehle, S., and Zickfield, K.: Global carbon and other Biogeochemical Cycles and Feedbacks, in: Climate Change 2021: The Physical Science Basis. Contribution of Working Group I to the Sixth Assessment Report of the Intergovernmental Panel on Climate Change edited by: Masson-Delmotte, V., P. Zhai, A. Pirani, S.L. Connors, C. Péan, S. Berger, N. Caud, Y. Chen, L. Goldfarb, M.I. Gomis, M. Huang, K. Leitzell, E. Lonnoy, J.B.R. Matthews, T.K. Maycock, T. Waterfield, O. Yelekçi, R. Yu, and Zhou, B., Cambridge University Press., In Press, 2021.

Carranza, M. M., and Gille, S. T.: Southern Ocean wind-driven entrainment enhances satellite chlorophyll-a through the summer, Journal of Geophysical Research-Oceans, 120, 304-323, 10.1002/2014jc010203, 2015.

Cavan, E. L., Henson, S. A., Belcher, A., and Sanders, R.: Role of zooplankton in determining the efficiency of the biological carbon pump, Biogeosciences, 14, 177-186, 2017.

Charalampopoulou, A., Poulton, A. J., Bakker, D. C. E., Lucas, M. I., Stinchcombe, M. C., and Tyrrell, T.: Environmental drivers of coccolithophore abundance and calcification across Drake Passage (Southern Ocean), Biogeosciences, 13, 5917-5935, 10.5194/bg-13-5917-2016, 2016.

Coggins, A., Watson, A. J., Schuster, U., Mackay, N., King, B., McDonagh, E., and Poulton, A. J.: Surface ocean carbon budget in the 2017 south Georgia diatom bloom: Observations and validation of profiling biogeochemical argo floats, Deep-Sea Res Pt Ii, 209, 105275, ARTN 105275

10.1016/j.dsr2.2023.105275, 2023.

Constable, A. J., Melbourne-Thomas, J., Corney, S. P., Arrigo, K. R., Barbraud, C., Barnes, D. K. A., Bindoff, N. L., Boyd, P. W., Brandt, A., Costa, D. P., Davidson, A. T., Ducklow, H. W., Emmerson, L., Fukuchi, M., Gutt, J., Hindell, M. A., Hofmann, E. E., Hosie, G. W., Iida, T., Jacob, S., Johnston, N. M., Kawaguchi, S., Kokubun, N., Koubbi, P., Lea, M.-A., Makhado, A., Massom, R. A., Meiners, K., Meredith, M. P., Murphy, E. J., Nicol, S., Reid, K., Richerson, K., Riddle, M. J., Rintoul, S. R., Smith Jr, W. O., Southwell, C., Stark, J. S., Sumner, M., Swadling, K. M., Takahashi, K. T., Trathan, P. N., Welsford, D. C., Weimerskirch, H., Westwood, K. J., Wienecke, B. C., Wolf-Gladrow, D., Wright, S. W., Xavier, J. C., and Ziegler, P.: Climate change and Southern Ocean ecosystems I: how changes in physical habitats directly affect marine biota, Global Change Biology, 20, 3004-3025, https://doi.org/10.1111/gcb.12623, 2014.

de Baar, H. J. W., de Jong, J. T. M., Bakker, D. C. E., Löscher, B. M., Veth, C., Bathmann, U., and Smetacek, V.: Importance of iron for plankton blooms and carbon dioxide drawdown in the Southern Ocean, Nature, 373, 412-415, 10.1038/373412a0, 1995.

Death, R., Wadham, J. L., Monteiro, F., Le Brocq, A. M., Tranter, M., Ridgwell, A., Dutkiewicz, S., and Raiswell, R.: Antarctic ice sheet fertilises the Southern Ocean, Biogeosciences, 11, 2635-2643, 10.5194/bg-11-2635-2014, 2014.

Deppeler, S. L., and Davidson, A. T.: Southern Ocean Phytoplankton in a Changing Climate, Frontiers in Marine Science, 4, ARTN 40

10.3389/fmars.2017.00040, 2017.

DeVries, T.: The oceanic anthropogenic CO2 sink: Storage, air-sea fluxes, and transports over the industrial era, Global Biogeochemical Cycles, 28, 631-647, 10.1002/2013gb004739, 2014.

Ducklow, H. W., Baker, K., Martinson, D. G., Quetin, L. B., Ross, R. M., Smith, R. C., Stammerjohn, S. E., Vernet, M., and Fraser, W.: Marine pelagic ecosystems: the west Antarctic Peninsula, Philos Trans R Soc Lond B Biol Sci, 362, 67-94, 10.1098/rstb.2006.1955, 2007.

Freeman, N. M., Lovenduski, N. S., Munro, D. R., Krumhardt, K. M., Lindsay, K., Long, M. C., and Maclennan, M.: The Variable and Changing Southern Ocean Silicate Front: Insights From the CESM Large Ensemble, Global Biogeochemical Cycles, 32, 752-768, 10.1029/2017gb005816, 2018.

Friedlingstein, P., Jones, M. W., O'Sullivan, M., Andrew, R. M., Bakker, D. C. E., Hauck, J., Le Quéré, C., Peters, G. P., Peters, W., Pongratz, J., Sitch, S., Canadell, J. G., Ciais, P., Jackson, R. B., Alin, S. R., Anthoni, P., Bates, N. R., Becker, M., Bellouin, N., Bopp, L., Chau, T. T. T., Chevallier, F., Chini, L. P., Cronin, M., Currie, K. I., Decharme, B., Djeutchouang, L. M., Dou, X. Y., Evans, W., Feely, R. A., Feng, L., Gasser, T., Gilfillan, D., Gkritzalis, T., Grassi, G., Gregor, L., Gruber, N., Gürses, Ö., Harris, I., Houghton, R. A., Hurtt, G. C., Iida, Y., Ilyina, T., Luijkx, I. T., Jain, A., Jones, S. D., Kato, E., Kennedy, D., Goldewijk, K. K., Knauer, J., Korsbakken, J. I., Körtzinger, A., Landschützer, P., Lauvset, S. K., Lefèvre, N., Lienert, S., Liu, J. J., Marland, G., McGuire, P. C., Melton, J. R., Munro, D. R., Nabel, J. E. M. S., Nakaoka, S. I., Niwa, Y., Ono, T., Pierrot, D., Poulter, B., Rehder, G., Resplandy, L., Robertson, E., Rödenbeck, C., Rosan, T. M., Schwinger, J., Schwingshackl, C., Séférian, R., Sutton, A. J., Sweeney, C., Tanhua, T., Tans, P. P., Tian, H. Q., Tilbrook, B., Tubiello, F., van der Werf, G. R., Vuichard, N., Wada, C., Wanninkhof, R., Watson, A. J., Willis, D., Wiltshire, A. J., Yuan, W. P., Yue, C., Yue, X., Zaehle, S., and Zeng, J. Y.: Global Carbon Budget 2021, Earth System Science Data, 14, 1917-2005, 10.5194/essd-14-1917-2022, 2022.

Frölicher, T. L., Sarmiento, J. L., Paynter, D. J., Dunne, J. P., Krasting, J. P., and Winton, M.: Dominance of the Southern Ocean in Anthropogenic Carbon and Heat Uptake in CMIP5 Models, Journal of Climate, 28, 862-886, 10.1175/jcli-d-14-00117.1, 2015.

Fu, W., Moore, J. K., Primeau, F., Collier, N., Ogunro, O. O., Hoffman, F. M., and Randerson, J. T.: Evaluation of Ocean Biogeochemistry and Carbon Cycling in CMIP Earth System Models With the International Ocean Model Benchmarking (IOMB) Software System, Journal of Geophysical Research: Oceans, 127, 10.1029/2022jc018965, 2022.

Fu, W. W., Randerson, J. T., and Moore, J. K.: Climate change impacts on net primary production (NPP) and export production (EP) regulated by increasing stratification and phytoplankton community structure in the CMIP5 models, Biogeosciences, 13, 5151-5170, 10.5194/bg-13-5151-2016, 2016.

Garcia, H., Weathers, K., Paver, C., Smolyar, I., Boyer, T., Locarnini, M., Zweng, M., Mishonov, A., Baranova, O., and Seidov, D.: World ocean atlas 2018. Vol. 4: Dissolved inorganic nutrients (phosphate, nitrate and nitrate+ nitrite, silicate), 2019.

Gregg, W. W., Conkright, M. E., Ginoux, P., O'Reilly, J. E., and Casey, N. W.: Ocean primary production and climate: Global decadal changes, Geophysical Research Letters, 30, Artn 1809

10.1029/2003gl016889, 2003.

Gregor, L., Kok, S., and Monteiro, P. M. S.: Interannual drivers of the seasonal cycle of CO2 in the Southern Ocean, Biogeosciences, 15, 2361-2378, 10.5194/bg-15-2361-2018, 2018.

Correctly calculating annual averages with Xarray: https://ncar.github.io/esds/posts/2021/yearly-averages-xarray/, access: 20/01/2024, 2021.

Gruber, N., Landschutzer, P., and Lovenduski, N. S.: The Variable Southern Ocean Carbon Sink, Ann Rev Mar Sci, 11, 159-186, 10.1146/annurev-marine-121916-063407, 2019.

Guidi, L., Chaffron, S., Bittner, L., Eveillard, D., Larhlimi, A., Roux, S., Darzi, Y., Audic, S., Berline, L., Brum, J., Coelho, L. P., Espinoza, J. C. I., Malviya, S., Sunagawa, S., Dimier, C., Kandels-Lewis, S., Picheral, M., Poulain, J., Searson, S., Tara Oceans, c., Stemmann, L., Not, F., Hingamp, P., Speich, S., Follows, M., Karp-Boss, L., Boss, E., Ogata, H., Pesant, S., Weissenbach, J., Wincker, P., Acinas, S. G., Bork, P., de Vargas, C., Iudicone, D., Sullivan, M. B., Raes, J., Karsenti, E., Bowler, C., and Gorsky, G.: Plankton networks driving carbon export in the oligotrophic ocean, Nature, 532, 465-470, 10.1038/nature16942, 2016.

Haberman, K. L., Ross, R. M., and Quetin, L. B.: Diet of the Antarctic krill (Euphausia superba Dana): II.: Selective grazing in mixed phytoplankton assemblages, Journal of Experimental Marine Biology and Ecology, 283, 97-113, 10.1016/S0022-0981(02)00467-7, 2003.

Hauck, J., Völker, C., Wolf-Gladrow, D. A., Laufkötter, C., Vogt, M., Aumont, O., Bopp, L., Buitenhuis, E. T., Doney, S. C., Dunne, J., Gruber, N., Hashioka, T., John, J., Le Quéré, C., Lima, I. D., Nakano, H., Séférian, R., and Totterdell, I.: On the Southern Ocean CO2 uptake and the role of the biological carbon pump in the 21st century, Global Biogeochemical Cycles, 29, 1451-1470, 10.1002/2015gb005140, 2015.

Heneghan, R. F., Everett, J. D., Blanchard, J. L., Sykes, P., and Richardson, A. J.: Climate-driven zooplankton shifts cause large-scale declines in food quality for fish, Nature Climate Change, 13, 470-477, 10.1038/s41558-023-01630-7, 2023.

Henley, S. F., Tuerena, R. E., Annett, A. L., Fallick, A. E., Meredith, M. P., Venables, H. J., Clarke, A., and Ganeshram, R. S.: Macronutrient supply, uptake and recycling in the coastal ocean of the west Antarctic Peninsula, Deep-Sea Res Pt Ii, 139, 58-76, 10.1016/j.dsr2.2016.10.003, 2017.

Henley, S. F., Schofield, O. M., Hendry, K. R., Schloss, I. R., Steinberg, D. K., Moffat, C., Peck, L. S., Costa, D. P., Bakker, D. C. E., Hughes, C., Rozema, P. D., Ducklow, H. W., Abele, D., Stefels, J., Van Leeuwe, M. A., Brussaard, C. P. D., Buma, A. G. J., Kohut, J., Sahade, R., Friedlaender, A. S., Stammerjohn, S. E., Venables, H. J., and Meredith, M. P.: Variability and change in the west Antarctic Peninsula marine system: Research priorities and opportunities, Progress in Oceanography, 173, 208-237, 10.1016/j.pocean.2019.03.003, 2019.

Henley, S. F., Cavan, E. L., Fawcett, S. E., Kerr, R., Monteiro, T., Sherrell, R. M., Bowie, A. R., Boyd, P. W., Barnes, D. K. A., Schloss, I. R., Marshall, T., Flynn, R., and Smith, S.: Changing Biogeochemistry of the Southern Ocean and Its Ecosystem Implications, Frontiers in Marine Science, 7, ARTN 581

10.3389/fmars.2020.00581, 2020.

Henson, S. A., Cael, B. B., Allen, S. R., and Dutkiewicz, S.: Future phytoplankton diversity in a changing climate, Nat Commun, 12, 5372, 10.1038/s41467-021-25699-w, 2021.

Henson, S. A., Laufkötter, C., Leung, S., Giering, S. L. C., Palevsky, H. I., and Cavan, E. L.: Uncertain response of ocean biological carbon export in a changing world, Nature Geoscience, 15, 248-254, 10.1038/s41561-022-00927-0, 2022.

Hudson, R. J., and Morel, F. M.: lron transport in marine phytoplankton: Kinetics of cellular and medium coordination reactions, Limnology and Oceanography, 35, 1002-1020, 1990.

Jabre, L. J., Allen, A. E., McCain, J. S. P., McCrow, J. P., Tenenbaum, N., Spackeen, J. L., Sipler, R. E., Green, B. R., Bronk, D. A., Hutchins, D. A., and Bertrand, E. M.: Molecular underpinnings and biogeochemical consequences of enhanced diatom growth in a warming Southern Ocean, Proc Natl Acad Sci U S A, 118, e2107238118, 10.1073/pnas.2107238118, 2021.

Jiang, L.-Q., Carter, B. R., Feely, R. A., Lauvset, S. K., and Olsen, A.: Surface ocean pH and buffer capacity: past, present and future, Sci Rep, 9, 18624, 10.1038/s41598-019-55039-4, 2019.

Jin, X., Gruber, N., Dunne, J. P., Sarmiento, J. L., and Armstrong, R. A.: Diagnosing the contribution of phytoplankton functional groups to the production and export of particulate organic carbon, CaCO3, and opal from global nutrient and alkalinity distributions, Global Biogeochemical Cycles, 20,

10.1029/2005gb002532, 2006.

Kang, S. H., Kang, J. S., Lee, S., Chung, K. H., Kim, D., and Park, M. G.: Antarctic phytoplankton assemblages in the marginal ice zone of the northwestern Weddell Sea, Journal of Plankton Research, 23, 333-352, DOI 10.1093/plankt/23.4.333, 2001.

Kawaguchi, S., Ishida, A., King, R., Raymond, B., Waller, N., Constable, A., Nicol, S., Wakita, M., and Ishimatsu, A.: Risk maps for Antarctic krill under projected Southern Ocean acidification, Nature Climate Change, 3, 843-847, 10.1038/Nclimate1937, 2013.

Kwiatkowski, L., Aumont, O., Bopp, L., and Ciais, P.: The Impact of Variable Phytoplankton Stoichiometry on Projections of Primary Production, Food Quality, and Carbon Uptake in the Global Ocean, Global Biogeochemical Cycles, 32, 516-528, 10.1002/2017gb005799, 2018.

Kwon, E. Y., Sreeush, M. G., Timmermann, A., Karl, D. M., Church, M. J., Lee, S.-S., and Yamaguchi, R.: Nutrient uptake plasticity in phytoplankton sustains future ocean net primary production, Science Advances, 8, eadd2475, doi:10.1126/sciadv.add2475, 2022.

Landschutzer, P., Gruber, N., Haumann, F. A., Rodenbeck, C., Bakker, D. C., van Heuven, S., Hoppema, M., Metzl, N., Sweeney, C., Takahashi, T., Tilbrook, B., and Wanninkhof, R.: The reinvigoration of the Southern Ocean carbon sink, Science, 349, 1221-1224, 10.1126/science.aab2620, 2015.

Lannuzel, D., Chever, F., van der Merwe, P. C., Janssens, J., Roukaerts, A., Cavagna, A. J., Townsend, A. T., Bowie, A. R., and Meiners, K. M.: Iron biogeochemistry in Antarctic pack ice during SIPEX-2, Deep-Sea Res Pt Ii, 131, 111-122, 10.1016/j.dsr2.2014.12.003, 2016.

Laufkötter, C., Vogt, M., Gruber, N., Aita-Noguchi, M., Aumont, O., Bopp, L., Buitenhuis, E., Doney, S. C., Dunne, J., and Hashioka, T.: Drivers and uncertainties of future global marine primary production in marine ecosystem models, Biogeosciences, 12, 6955-6984, 2015.

Leung, S., Cabré, A., and Marinov, I.: A latitudinally banded phytoplankton response to 21st century climate change in the Southern Ocean across the CMIP5 model suite, Biogeosciences, 12, 5715-5734, 10.5194/bg-12-5715-2015, 2015.

Lewandowska, A. M., Hillebrand, H., Lengfellner, K., and Sommer, U.: Temperature effects on phytoplankton diversity - The zooplankton link, Journal of Sea Research, 85, 359-364, 10.1016/j.seares.2013.07.003, 2014.

Litchman, E., and Klausmeier, C. A.: Trait-Based Community Ecology of Phytoplankton, Annual Review of Ecology Evolution and Systematics, 39, 615-639, 10.1146/annurev.ecolsys.39.110707.173549, 2008.

Llort, J., Lévy, M., Sallée, J. B., and Tagliabue, A.: Nonmonotonic Response of Primary Production and Export to Changes in Mixed-Layer Depth in the Southern Ocean, Geophysical Research Letters, 46, 3368-3377, 10.1029/2018gl081788, 2019.

Long, M. C., Moore, J. K., Lindsay, K., Levy, M., Doney, S. C., Luo, J. Y., Krumhardt, K. M., Letscher, R. T., Grover, M., and Sylvester, Z. T.: Simulations With the Marine Biogeochemistry Library (MARBL), Journal of Advances in Modeling Earth Systems, 13, e2021MS002647, ARTN e2021MS002647

10.1029/2021MS002647, 2021.

Lopez-Urrutia, A., San Martin, E., Harris, R. P., and Irigoien, X.: Scaling the metabolic balance of the oceans, Proc Natl Acad Sci U S A, 103, 8739-8744, 10.1073/pnas.0601137103, 2006.

Luo, Y. W., Doney, S. C., Anderson, L. A., Benavides, M., Berman-Frank, I., Bode, A., Bonnet, S., Boström, K. H., Böttjer, D., Capone, D. G., Carpenter, E. J., Chen, Y. L., Church, M. J., Dore, J. E., Falcón, L. I., Fernández, A., Foster, R. A., Furuya, K., Gómez, F., Gundersen, K., Hynes, A. M., Karl, D. M., Kitajima, S., Langlois, R. J., LaRoche, J., Letelier, R. M., Marañón, E., McGillicuddy, D. J., Moisander, P. H., Moore, C. M., Mourino-Carballido, B., Mulholland, M. R., Needoba, J. A., Orcutt, K. M., Poulton, A. J., Rahav, E., Raimbault, P., Rees, A. P., Riemann, L., Shiozaki, T., Subramaniam, A., Tyrrell, T., Turk-Kubo, K. A., Varela, M., Villareal, T. A., Webb, E. A., White, A. E., Wu, J., and Zehr, J. P.: Database of diazotrophs in global ocean: abundance, biomass and nitrogen fixation rates, Earth System Science Data, 4, 47-73, 10.5194/essd-4-47-2012, 2012.

Mascioni, M., Almandoz, G. O., Cefarelli, A. O., Cusick, A., Ferrario, M. E., and Vernet, M.: Phytoplankton composition and bloom formation in unexplored nearshore waters of the western Antarctic Peninsula, Polar Biology, 42, 1859-1872, 10.1007/s00300-019-02564-7, 2019.

Masson-Delmotte, V., Zhai, P., Pirani, A., Connors, S. L., Péan, C., Berger, S., Caud, N., Chen, Y., Goldfarb, L., and Gomis, M.: Climate change 2021: the physical science basis, Contribution of working group I to the sixth assessment report of the intergovernmental panel on climate change, 2, 2021.

Matsuoka, K., Skoglund, A., Roth, G., de Pomereu, J., Griffiths, H., Headland, R., Herried, B., Katsumata, K., Le Brocq, A., Licht, K., Morgan, F., Neff, P. D., Ritz, C., Scheinert, M., Tamura, T., Van de Putte, A., van den Broeke, M., von Deschwanden, A., Deschamps-Berger, C., Van Liefferinge, B., Tronstad, S., and Melvær, Y.: Quantarctica, an integrated mapping environment for Antarctica, the Southern Ocean, and sub-Antarctic islands, Environmental Modelling & Software, 140, 105015, ARTN 105015

10.1016/j.envsoft.2021.105015, 2021.

Mayzaud, P., and Pakhomov, E. A.: The role of zooplankton communities in carbon recycling in the Ocean: the case of the Southern Ocean, Journal of Plankton Research, 36, 1543-1556, 10.1093/plankt/fbu076, 2014.

Mendes, C. R. B., Costa, R. R., Ferreira, A., Jesus, B., Tavano, V. M., Dotto, T. S., Leal, M. C., Kerr, R., Islabao, C. A., Franco, A., Mata, M. M., Garcia, C. A. E., and Secchi, E. R.: Cryptophytes: An emerging algal group in the rapidly changing Antarctic Peninsula marine environments, Glob Chang Biol, 29, 1791-1808, 10.1111/gcb.16602, 2023.

Meredith, M., Sommerkorn, M., Cassotta, S., Derksen, C., Ekaykin, A., Hollowed, A., Kofinas, G., Mackintosh, A., Melbourne-Thomas, J., and Muelbert, M.: Chapter 3: polar regions, IPCC special report on the ocean and cryosphere in a changing climate, 5, 2019.

Moline, M. A., Claustre, H., Frazer, T. K., Schofield, O., and Vernet, M.: Alteration of the food web along the Antarctic Peninsula in response to a regional warming trend, Global Change Biology, 10, 1973-1980, 10.1111/j.1365-2486.2004.00825.x, 2004.

Moline, M. A., Karnovsky, N. J., Brown, Z., Divoky, G. J., Frazer, T. K., Jacoby, C. A., Torrese, J. J., and Fraser, W. R.: High latitude changes in ice dynamics and their impact on polar marine ecosystems, Year in Ecology and Conservation Biology 2008, 1134, 267-319, 10.1196/annals.1439.010, 2008.

Montes-Hugo, M. A., Vernet, M., Martinson, D., Smith, R., and Iannuzzi, R.: Variability on phytoplankton size structure in the western Antarctic Peninsula (1997-2006), Deep-Sea Res Pt Ii, 55, 2106-2117, 10.1016/j.dsr2.2008.04.036, 2008.

Moore, C. M., Mills, M. M., Arrigo, K. R., Berman-Frank, I., Bopp, L., Boyd, P. W., Galbraith, E. D., Geider, R. J., Guieu, C., Jaccard, S. L., Jickells, T. D., La Roche, J., Lenton, T. M., Mahowald, N. M., Marañón, E., Marinov, I., Moore, J. K., Nakatsuka, T., Oschlies, A., Saito, M. A., Thingstad, T. F., Tsuda, A., and Ulloa, O.: Processes and patterns of oceanic nutrient limitation, Nature Geoscience, 6, 701-710, 10.1038/Ngeo1765, 2013.

Moore, J. K., Doney, S. C., and Lindsay, K.: Upper ocean ecosystem dynamics and iron cycling in a global three-dimensional model, Global Biogeochemical Cycles, 18, Artn Gb4028

10.1029/2004gb002220, 2004.

Moreau, S., Mostajir, B., Belanger, S., Schloss, I. R., Vancoppenolle, M., Demers, S., and Ferreyra, G. A.: Climate change enhances primary production in the western Antarctic Peninsula, Glob Chang Biol, 21, 2191-2205, 10.1111/gcb.12878, 2015.

Moreau, S., Boyd, P. W., and Strutton, P. G.: Remote assessment of the fate of phytoplankton in the Southern Ocean sea-ice zone, Nat Commun, 11, 3108, 10.1038/s41467-020-16931-0, 2020.

Moreau, S., Hattermann, T., de Steur, L., Kauko, H. M., Ahonen, H., Ardelan, M., Assmy, P., Chierici, M., Descamps, S., Dinter, T., Falkenhaug, T., Fransson, A., Gronningsaeter, E., Hallfredsson, E. H., Huhn, O., Lebrun, A., Lowther, A., Lubcker, N., Monteiro, P., Peeken, I., Roychoudhury, A., Rozanska, M., Ryan-Keogh, T., Sanchez, N., Singh, A., Simonsen, J. H., Steiger, N., Thomalla, S. J., van Tonder, A., Wiktor, J. M., and Steen, H.: Wind-driven upwelling of iron sustains dense blooms and food webs in the eastern Weddell Gyre, Nat Commun, 14, 1303, 10.1038/s41467-023-36992-1, 2023.

Nissen, C., Vogt, M., Münnich, M., Gruber, N., and Haumann, F. A.: Factors controlling coccolithophore biogeography in the Southern Ocean, Biogeosciences, 15, 6997-7024, 10.5194/bg-15-6997-2018, 2018.

O'Neill, B. C., Tebaldi, C., van Vuuren, D. P., Eyring, V., Friedlingstein, P., Hurtt, G., Knutti, R., Kriegler, E., Lamarque, J. F., Lowe, J., Meehl, G. A., Moss, R., Riahi, K., and Sanderson, B. M.: The Scenario Model Intercomparison Project (ScenarioMIP) for CMIP6, Geoscientific Model Development, 9, 3461-3482, 10.5194/gmd-9-3461-2016, 2016.

Pausch, F., Bischof, K., and Trimborn, S.: Iron and manganese co-limit growth of the Southern Ocean diatom Chaetoceros debilis, PLoS One, 14, e0221959, 10.1371/journal.pone.0221959, 2019.

Pearce, I., Davidson, A. T., Thomson, P. G., Wright, S., and van den Enden, R.: Marine microbial ecology in the sub-Antarctic Zone: Rates of bacterial and phytoplankton growth and grazing by heterotrophic protists, Deep-Sea Res Pt Ii, 58, 2248-2259, 10.1016/j.dsr2.2011.05.030, 2011.

Person, R., Aumont, O., and Lévy, M.: The Biological Pump and Seasonal Variability of pCO2 in the Southern Ocean: Exploring the Role of Diatom Adaptation to Low Iron, Journal of Geophysical Research-Oceans, 123, 3204-3226, 10.1029/2018jc013775, 2018.

Petrou, K., Baker, K. G., Nielsen, D. A., Hancock, A. M., Schulz, K. G., and Davidson, A. T.: Acidification diminishes diatom silica production in the Southern Ocean, Nature Climate Change, 9, 781-+, 10.1038/s41558-019-0557-y, 2019.

Purich, A., and England, M. H.: Historical and Future Projected Warming of Antarctic Shelf Bottom Water in CMIP6 Models, Geophysical Research Letters, 48, e2021GL092752, ARTN e2021GL092752

10.1029/2021GL092752, 2021.

Quéguiner, B.: Iron fertilization and the structure of planktonic communities in high nutrient regions of the Southern Ocean, Deep Sea Research Part II: Topical Studies in Oceanography, 90, 43-54, 10.1016/j.dsr2.2012.07.024, 2013.

Raphael, M. N., and Handcock, M. S.: A new record minimum for Antarctic sea ice, Nature Reviews Earth & Environment, 3, 215-216, 10.1038/s43017-022-00281-0, 2022.

Ratnarajah, L., Abu-Alhaija, R., Atkinson, A., Batten, S., Bax, N. J., Bernard, K. S., Canonico, G., Cornils, A., Everett, J. D., Grigoratou, M., Ishak, N. H. A., Johns, D., Lombard, F., Muxagata, E., Ostle, C., Pitois, S., Richardson, A. J., Schmidt, K., Stemmann, L., Swadling, K. M., Yang, G., and Yebra, L.: Monitoring and modelling marine zooplankton in a changing climate, Nature Communications, 14, 564, 10.1038/s41467-023-36241-5, 2023.

Riebesell, U., Schulz, K. G., Bellerby, R. G., Botros, M., Fritsche, P., Meyerhofer, M., Neill, C., Nondal, G., Oschlies, A., Wohlers, J., and Zollner, E.: Enhanced biological carbon consumption in a high CO2 ocean, Nature, 450, 545-548, 10.1038/nature06267, 2007.

Roach, L. A., Dörr, J., Holmes, C. R., Massonnet, F., Blockley, E. W., Notz, D., Rackow, T., Raphael, M. N., O'Farrell, S. P., Bailey, D. A., and Bitz, C. M.: Antarctic Sea Ice Area in CMIP6, Geophysical Research Letters, 47, e2019GL086729, ARTN e2019GL086729

10.1029/2019GL086729, 2020.

Rohr, T., Richardson, A. J., Lenton, A., Chamberlain, M. A., and Shadwick, E. H.: Zooplankton grazing is the largest source of uncertainty for marine carbon cycling in CMIP6 models, Communications Earth & Environment, 4, 212, 10.1038/s43247-023-00871-w, 2023.

Rozema, P. D., Venables, H. J., van de Poll, W. H., Clarke, A., Meredith, M. P., and Buma, A. G. J.: Interannual variability in phytoplankton biomass and species composition in northern Marguerite Bay (West Antarctic Peninsula) is governed by both winter sea ice cover and summer stratification, Limnology and Oceanography, 62, 235-252, 10.1002/lno.10391, 2017.

Saba, G. K., Fraser, W. R., Saba, V. S., Iannuzzi, R. A., Coleman, K. E., Doney, S. C., Ducklow, H. W., Martinson, D. G., Miles, T. N., Patterson-Fraser, D. L., Stammerjohn, S. E., Steinberg, D. K., and Schofield, O. M.: Winter and spring controls on the summer food web of the coastal West Antarctic Peninsula, Nat Commun, 5, 4318, 10.1038/ncomms5318, 2014.

Sallee, J. B., Pellichero, V., Akhoudas, C., Pauthenet, E., Vignes, L., Schmidtko, S., Garabato, A. N., Sutherland, P., and Kuusela, M.: Summertime increases in upper-ocean stratification and mixed-layer depth, Nature, 591, 592-598, 10.1038/s41586-021-03303-x, 2021.

Sarmiento, J. L., Gruber, N., Brzezinski, M. A., and Dunne, J. P.: High-latitude controls of thermocline nutrients and low latitude biological productivity, Nature, 427, 56-60, 10.1038/nature02127, 2004.

Sathyendranath, S., Stuart, V., Nair, A., Oka, K., Nakane, T., Bouman, H., Forget, M. H., Maass, H., and Platt, T.: Carbon-to-chlorophyll ratio and growth rate of phytoplankton in the sea, Marine Ecology Progress Series, 383, 73-84, 10.3354/meps07998, 2009.

Schofield, O., Brown, M., Kohut, J., Nardelli, S., Saba, G., Waite, N., and Ducklow, H.: Changes in the upper ocean mixed layer and phytoplankton productivity along the West Antarctic Peninsula, Philos Trans A Math Phys Eng Sci, 376, 20170173, 10.1098/rsta.2017.0173, 2018.

Seferian, R., Berthet, S., Yool, A., Palmieri, J., Bopp, L., Tagliabue, A., Kwiatkowski, L., Aumont, O., Christian, J., Dunne, J., Gehlen, M., Ilyina, T., John, J. G., Li, H., Long, M. C., Luo, J. Y., Nakano, H., Romanou, A., Schwinger, J., Stock, C., Santana-Falcon, Y., Takano, Y., Tjiputra, J., Tsujino, H., Watanabe, M., Wu, T., Wu, F., and Yamamoto, A.: Tracking Improvement in Simulated Marine Biogeochemistry Between CMIP5 and CMIP6, Curr Clim Change Rep, 6, 95-119, 10.1007/s40641-020-00160-0, 2020.

Shu, Q., Wang, Q., Song, Z. Y., Qiao, F. L., Zhao, J. C., Chu, M., and Li, X. F.: Assessment of Sea Ice Extent in CMIP6 With Comparison to Observations and CMIP5, Geophysical Research Letters, 47, e2020GL087965, ARTN e2020GL087965

10.1029/2020GL087965, 2020.

Steiner, N. S., Bowman, J., Campbell, K., Chierici, M., Eronen-Rasimus, E., Falardeau, M., Flores, H., Fransson, A., Herr, H., and Insley, S. J.: Climate change impacts on sea-ice ecosystems and associated ecosystem services, Elem Sci Anth, 9, 00007, 2021.

Stock, C. A., Dunne, J. P., and John, J. G.: Global-scale carbon and energy flows through the marine planktonic food web: An analysis with a coupled physical–biological model, Progress in Oceanography, 120, 1-28, 2014.

Stock, C. A., Dunne, J. P., Fan, S. M., Ginoux, P., John, J., Krasting, J. P., Laufkötter, C., Paulot, F., and Zadeh, N.: Ocean Biogeochemistry in GFDL's Earth System Model 4.1 and Its Response to Increasing Atmospheric CO2, Journal of Advances in Modeling Earth Systems, 12, e2019MS002043, ARTN e2019MS002043

10.1029/2019MS002043, 2020.

Strzepek, R. F., and Harrison, P. J.: Photosynthetic architecture differs in coastal and oceanic diatoms, Nature, 431, 689-692, 10.1038/nature02954, 2004.

Sunagawa, S., Acinas, S. G., Bork, P., Bowler, C., Tara Oceans, C., Eveillard, D., Gorsky, G., Guidi, L., Iudicone, D., Karsenti, E., Lombard, F., Ogata, H., Pesant, S., Sullivan, M. B., Wincker, P., and de Vargas, C.: Tara Oceans: towards global ocean ecosystems biology, Nat Rev Microbiol, 18, 428-445, 10.1038/s41579-020-0364-5, 2020.

Swadling, K. M., Constable, A. J., Fraser, A. D., Massom, R. A., Borup, M. D., Ghigliotti, L., Granata, A., Guglielmo, L., Johnston, N. M., Kawaguchi, S., Kennedy, F., Kiko, R., Koubbi, P., Makabe, R., Martin, A., McMinn, A., Moteki, M., Pakhomov, E. A., Peeken, I., Reimer, J., Reid, P., Ryan, K. G., Vacchi, M., Virtue, P., Weldrick, C. K., Wongpan, P., and Wotherspoon, S. J.: Biological responses to change in Antarctic sea ice habitats, Frontiers in Ecology and Evolution, 10, ARTN 1073823

10.3389/fevo.2022.1073823, 2023.

Tagliabue, A., Aumont, O., DeAth, R., Dunne, J. P., Dutkiewicz, S., Galbraith, E., Misumi, K., Moore, J. K., Ridgwell, A., Sherman, E., Stock, C., Vichi, M., Völker, C., and Yool, A.: How well do global ocean biogeochemistry models simulate dissolved iron distributions?, Global Biogeochemical Cycles, 30, 149-174, 10.1002/2015gb005289, 2016.

Tagliabue, A., Kwiatkowski, L., Bopp, L., Butenschön, M., Cheung, W., Lengaigne, M., and Vialard, J.: Persistent Uncertainties in Ocean Net Primary Production Climate Change Projections at Regional Scales Raise Challenges for Assessing Impacts on Ecosystem Services, Frontiers in Climate, 3, ARTN 738224

10.3389/fclim.2021.738224, 2021.

Timmermans, K. R., van der Wagt, B., and de Baar, H. J. W.: Growth rates, half-saturation constants, and silicate, nitrate, and phosphate depletion in relation to iron availability of four large, open-ocean diatoms from the Southern Ocean, Limnology and Oceanography, 49, 2141-2151, DOI 10.4319/lo.2004.49.6.2141, 2004.

Tortell, P. D., Payne, C. D., Li, Y., Trimborn, S., Rost, B., Smith, W. O., Riesselman, C., Dunbar, R. B., Sedwick, P., and DiTullio, G. R.: CO2 sensitivity of Southern Ocean phytoplankton, Geophysical Research Letters, 35, 10.1029/2007gl032583, 2008.

Touzé-Peiffer, L., Barberousse, A., and Le Treut, H.: The Coupled Model Intercomparison Project: History, uses, and structural effects on climate research, Wiley Interdisciplinary Reviews: Climate Change, 11, e648, 2020.

Tréguer, P., Bowler, C., Moriceau, B., Dutkiewicz, S., Gehlen, M., Aumont, O., Bittner, L., Dugdale, R., Finkel, Z., Iudicone, D., Jahn, O., Guidi, L., Lasbleiz, M., Leblanc, K., Levy, M., and Pondaven, P.: Influence of diatom diversity on the ocean biological carbon pump, Nature Geoscience, 11, 27-37, 10.1038/s41561-017-0028-x, 2017.

Turner, J., and Comiso, J.: Solve Antarctica's sea-ice puzzle, Nature, 547, 275-277, 10.1038/547275a, 2017.

Turner, J., Holmes, C., Harrison, T. C., Phillips, T., Jena, B., Reeves-Francois, T., Fogt, R., Thomas, E. R., and Bajish, C. C.: Record Low Antarctic Sea Ice Cover in February 2022, Geophysical Research Letters, 49, e2022GL098904, ARTN e2022GL098904

10.1029/2022GL098904, 2022.

Venables, H. J., Clarke, A., and Meredith, M. P.: Wintertime controls on summer stratification and productivity at the western Antarctic Peninsula, Limnology and Oceanography, 58, 1035-1047, 10.4319/lo.2013.58.3.1035, 2013.

Virtanen, P., Gommers, R., Oliphant, T. E., Haberland, M., Reddy, T., Cournapeau, D., Burovski, E., Peterson, P., Weckesser, W., and Bright, J.: SciPy 1.0: fundamental algorithms for scientific computing in Python, Nature methods, 17, 261-272, 2020.

Ward, B. A., and Follows, M. J.: Marine mixotrophy increases trophic transfer efficiency, mean organism size, and vertical carbon flux, Proc Natl Acad Sci U S A, 113, 2958-2963, 10.1073/pnas.1517118113, 2016.

Watson, A. J., Bakker, D. C., Ridgwell, A. J., Boyd, P. W., and Law, C. S.: Effect of iron supply on Southern Ocean CO2 uptake and implications for glacial atmospheric CO2, Nature, 407, 730-733, 10.1038/35037561, 2000.

Wright, S. W., van den Enden, R. L., Pearce, I., Davidson, A. T., Scott, F. J., and Westwood, K. J.: Phytoplankton community structure and stocks in the Southern Ocean (30–80 E) determined by CHEMTAX analysis of HPLC pigment signatures, Deep Sea Research Part II: Topical Studies in Oceanography, 57, 758-778, 2010.

Xu, K., Fu, F. X., and Hutchins, D. A.: Comparative responses of two dominant Antarctic phytoplankton taxa to interactions between ocean acidification, warming, irradiance, and iron availability, Limnology and Oceanography, 59, 1919-1931, 10.4319/lo.2014.59.6.1919, 2014.

Zhu, Z., Xu, K., Fu, F. X., Spackeen, J. L., Bronk, D. A., and Hutchins, D. A.: A comparative study of iron and temperature interactive effects on diatoms and Phaeocystis antarctica from the Ross Sea, Antarctica, Marine Ecology Progress Series, 550, 39-51, 10.3354/meps11732, 2016.

Zhuang, J., Dussin, R., Jüling, A., and Rasp, S.: xESMF: Universal regridder for geospatial data, Zenodo [code], 10, 2018.